


Superconformal anomalies for string defects in six-dimensional $\mathcal{N} = (1, 0)$ SCFTs

Fabio Apruzzi ^{a,b} Noppadol Mekareeya ^{c,d} Brandon Robinson ^c
 and Alessandro Tomasiello ^{c,e}

^a*Dipartimento di Fisica e Astronomia “Galileo Galilei”, Università di Padova,
Via Marzolo 8, 35131 Padova, Italy*

^b*INFN, Sezione di Padova Via Marzolo 8, 35131 Padova, Italy*

^c*INFN, Sezione di Milano-Bicocca,
Piazza della Scienza 3, I-20126 Milano, Italy*

^d*Department of Physics, Faculty of Science, Chulalongkorn University,
Phayathai Road, Pathumwan, Bangkok 10330, Thailand*

^e*Dipartimento di Matematica, Università di Milano Bicocca,
Via Cozzi 55, 20126 Milano, Italy*

E-mail: fabio.apruzzi@pd.infn.it, n.mekareeya@gmail.com,
brandon.robinson@mib.infn.it, alessandro.tomasiello@unimib.it

ABSTRACT: We study the anomalies of two-dimensional BPS defects in six-dimensional $\mathcal{N} = (1, 0)$ superconformal field theories. Using a holographic description of these defects furnished by probe D4-branes in AdS₇ solutions of ten-dimensional type IIA supergravity, we compute the two independent defect Weyl anomalies from the on-shell action for a spherical defect and defect sphere entanglement entropy. We find agreement between the holographic prediction for the defect A-type anomaly coming from the defect sphere free energy and the leading large N contribution to the defect ’t Hooft anomaly found using anomaly inflow. We also find agreement between the holographic computation of the expectation value of a surface operator wrapping a torus and the supersymmetric localization computation for a circular Wilson loop in $\mathcal{N} = 1$ super Yang-Mills theory on S⁵. Lastly, we holographically compute the defect gravitational anomaly from the Wess-Zumino action of the probe D4-brane, which provides a subleading large N correction to the defect A-type anomaly.

KEYWORDS: AdS-CFT Correspondence, Supersymmetric Gauge Theory, Anomalies in Field and String Theories

ARXIV EPRINT: [2407.18049](https://arxiv.org/abs/2407.18049)

Contents

1	Introduction	1
2	AdS₇/CFT₆	4
3	Probe brane holography	6
3.1	Probe D4-brane embedding	6
3.2	Spherical entanglement entropy	8
3.3	On-shell action	11
3.4	Defect gravitational anomaly	14
4	Anomalies from field theory and their string theory constructions	16
4.1	Necklace quivers and supersymmetry localization on S ⁵	16
4.2	Anomaly inflow from type IIB	18
5	Discussion	22
A	Coordinate transformations	23
B	Two-dimensional quiver gauge theories	25

1 Introduction

Among the powerful holographic tools available to study gauge theories at strong coupling, probe brane holography provides a controlled framework with which to systematically introduce heavy charged operators [1] or submanifold localized degrees of freedom [2, 3] in a regime where the number of operators holographically sourced by the probe brane remains parametrically small compared to the number of color degrees of freedom. By carefully constructing the brane embedding to preserve supersymmetry on the intersection of the curved conformal boundary of the ambient AdS space and the brane worldvolume, probe brane holography has passed a number of precision tests through comparison to results obtained by supersymmetric localization [4–6]. On the gravity side, taking the probe limit of a brane embedding includes taking the brane tension to be parametrically large, which to leading order freezes out the probe brane’s gravitational degrees of freedom and suppresses backreaction onto the background geometry. This limit greatly simplifies the computation of key physical quantities that characterize probe brane degrees of freedom such as the brane’s on-shell action and contributions to Entanglement Entropy (EE), both of which will be the primary focus of our holographic computations.

In the study of superconformal field theories (SCFTs), the $d = 6$ case has a distinguished role. It is the highest dimension in which SCFTs exist; moreover, six-dimensional (6d) theories spawn a large variety of theories in lower dimensions. The most famous example is the $\mathcal{N} = (2, 0)$ theory on M5-brane stacks [7], but a lot more examples exist with $\mathcal{N} = (1, 0)$,

engineered by orbifolds, M-theory walls, F-theory, IIA brane intersections [8–11]. The latter also have holographic duals, the $\text{AdS}_7 \times M_3$ solutions in massive IIA [12–14].

Codimension-two defects in 6d SCFTs have played a role in their compactifications down to four dimensions, appearing as punctures on an internal Riemann surface; see for example [15–18]. On the other hand, codimension-four defects have been studied much less. In $\mathcal{N} = (2, 0)$ theories these defects are provided by M2-branes [19–21] and can be distinguished from the other codimension-four degrees of freedom, i.e. tensionless strings, by how they fit in to the defect group of the theory [22]. In this paper we initiate the study of codimension-four defects in the much more numerous $\mathcal{N} = (1, 0)$ theories.

Similar to ordinary standalone CFTs, conformal defects (DCF_Ts) can be partially characterized by data expressed in the form of anomalies, e.g. for defect R-symmetry or Weyl symmetry. Moreover, defect anomalies, like in their CFT counterparts, have long been known to appear in the correlation functions of protected operators in the spectrum, e.g. the displacement operator [23], and in other physical observables, e.g. defect transport and heat capacity [24], and so are crucial quantities of study in many areas of physics [25]. Thus, computing these defect anomaly data — both the defect R- and Weyl anomalies — gives us robust information about the defect degrees of freedom and their physics for a novel class of extended operators in strongly coupled 6d SCFTs with no known Lagrangian description. We do this by using a combination of anomaly inflow, supersymmetric localization, and probe brane holography. In particular, the anomaly inflow computation has been successful in capturing anomalies of tensionless strings of 6d theories, as well as anomalies of codimension two defects of $\mathcal{N} = (2, 0)$ 6d theories, such as punctures [26]. We refine the inflow mechanism in presence of codimension four defects, hence providing a novel example of anomaly inflow of such kind. Additionally, since there are an infinite family of lower dimensional theories obtainable by partially twisted dimensional reduction of the ambient 6d theories that host the defect systems we study, the computation of the anomalies of string-like defects in 6d theories provides important information for a large class of deformations of 4d and 3d QFTs, see e.g. [19]. Further for the defect systems that we study, the additional constraints provided by preserving some amount of the ambient supersymmetries gives us a set of non-perturbative formulae that connect the defect ‘t Hooft and Weyl anomalies, which will allow for precision checks on our computations.

The generic form for the Weyl anomaly of a (super)conformal defect supported on a two-dimensional submanifold, Σ , embedded a d -dimensional ambient space is¹

$$T^\mu{}_\mu|_\Sigma = \frac{1}{24\pi} (a_\Sigma \bar{E}_2 + d_1 \mathring{\mathbb{I}}^2 + d_2 P[W]_\Sigma) \tag{1.1}$$

where \bar{E}_2 is the two-dimensional Euler density built from the intrinsic metric of the defect submanifold, $\mathring{\mathbb{I}}^2$ is the square of the trace-free second fundamental form for the embedding, and $P[W]_\Sigma$ is the trace of the pullback of the ambient Weyl tensor to the defect. The A-type [28] defect Weyl anomaly a_Σ has been shown to obey a weak c-theorem [29, 30] and, with a sufficient amount of supersymmetry preserved on the defect, to be related to defect R- and gravitational anomalies [30]. The B-type anomalies d_1 and d_2 are strictly non-negative in

¹Since our focus is on co-dimension four defects, there are only parity even defect anomalies [27].

reflection positive theories [27, 31], but do not obey any known c-theorem. However, relevant to the cases we are interested, it is known that $d_1 = d_2$ for two-dimensional conformal defect preserving at least $\mathcal{N} = (2, 0)$ defect supersymmetry [32, 33], and so in order to characterize BPS string defects in six-dimensional $\mathcal{N} = (1, 0)$ SCFTs, we only need to compute a_Σ and d_2 . Crucial for our analysis below, these defect anomalies are known to control two quantities that can be easily computed using probe brane holography: the log divergent part of defect sphere free energy, which is uniquely determined by a_Σ , and the universal part of the defect sphere EE, which is fixed by a linear combination of a_Σ and d_2 [27, 34].

In section 2, we briefly review AdS₇ solutions to type IIA SUGRA found in [12–14] and their holographic dual description in terms of six-dimensional $\mathcal{N} = (1, 0)$ SCFT at large N .

In section 3, we construct solutions for embedding probe D4-brane into a generic AdS₇ × M₃ background with non-trivial Romans mass.² Further in this section, we carry out four holographic computations that characterize the two-dimensional defect in the field theory. First, we compute the defect contribution to the EE of a spherical region. Second, we compute the a_Σ anomaly from the free energy of a spherical defect and use the defect EE result to obtain the B-type anomalies. In terms of the number of probe D4-branes q_i and partitions of D6-branes r_i they can be succinctly written to leading order in large N as

$$a_\Sigma = 24(q, r), \quad d_1 = d_2 = 32(q, r) \tag{1.2}$$

with scalar product taken with respect to the inverse Cartan matrix of A_{N-1} . Third, we holographically compute the expectation value of the string defect operator W on $\mathbb{S}_{\beta/4\pi}^1 \times \mathbb{S}^1$, which gives

$$\langle W \rangle = \exp[\beta(q, r)]. \tag{1.3}$$

Lastly, we compute the defect gravitational anomaly from the Wess-Zumino action, which is shown to be subleading at large N and contributes to the a_Σ anomaly

$$a_\Sigma = 24(q, r) + \frac{1}{2} \sum_i q_i r_i. \tag{1.4}$$

In section 4, we compare the probe brane results to anomalies computed via other means. In section 4.1, we compare the expectation value of the torus Wilson surface to the dimensionally reduced circular Wilson loop obtained purely in field theory using supersymmetric localization of $\mathcal{N} = 1$ SYM theory on \mathbb{S}^5 . Despite the holographic computation only computing the value at large N and the supersymmetric localization result being exact, we find a precise match between the two expressions. Later, in section 4.2, we consider the type IIB description of string defects in six-dimensional SCFTs. By the help of these string constructions we study the 6d anomaly polynomial inflow onto the defect. In particular, we compute the defect R-anomaly and successfully match the leading large N result for the a_Σ anomaly. As a byproduct we developed the inflow mechanism for (string) defects provided by probe branes in IIB backgrounds engineering 6d SCFTs. This approach could be potentially generalized to other type (non-string) of defects.

²Some fully back-reacted solutions for codimension-four defects exist [35–38], and it would be interesting to compare our approach to those results; the AdS₃ × S³ solutions appear particularly relevant.

In appendix A, we explain the coordinate transformations used in section 3.1. In appendix B, we consider a purely two-dimensional description of the D2-D4-D6 brane system in terms of a quiver gauge theory. We demonstrate that the quiver description correctly captures the subleading large N contributions (only) to the defect anomaly, i.e. the gravitational anomaly. Differently from the BPS strings, which become tensionless at the fixed point, the quiver which includes the defect does not capture the full defect degrees of freedom. We argue that the quiver only provides the intrinsic degrees of freedom of the defect. However it does not capture the bulk-defect ones, which are instead computed via anomaly inflow.

2 AdS₇/CFT₆

The starting point is the asymptotically AdS₇ × M₃ background solutions to type IIA SUGRA constructed in [12–14]

$$\begin{aligned} \frac{1}{\pi\sqrt{2}}ds^2 &= 8\sqrt{-\frac{\alpha}{\alpha''}}ds_7^2 + \sqrt{-\frac{\alpha''}{\alpha}}\left(dz^2 + \frac{\alpha^2}{\alpha'^2 - 2\alpha\alpha''}d\Omega_2^2\right), \\ e^\phi &= 3^4\left(\sqrt{2\pi}\right)^{\frac{5}{2}}\frac{(-\alpha/\alpha'')^{\frac{3}{4}}}{\sqrt{\alpha'^2 - 2\alpha\alpha''}}, \\ B &= \pi\left(-z + \frac{\alpha\alpha'}{\alpha'^2 - 2\alpha\alpha''}\right)\text{vol}_{\mathbb{S}^2}, \\ F_2 &= \left(\frac{\alpha''}{162\pi^2} + \frac{\pi F_0\alpha\alpha'}{\alpha'^2 - 2\alpha\alpha''}\right)\text{vol}_{\mathbb{S}^2}. \end{aligned} \tag{2.1}$$

Here ds_7^2 is the line element on AdS₇, $d\Omega_2^2$ is the line element on the unit 2-sphere \mathbb{S}^2 , prime denotes ∂_z , and α is a C^1 piecewise-cubic function on the interval $z \in [0, N]$ that satisfies $\alpha > 0$, $\alpha'' < 0$,

$$\alpha'''(z) = -162\pi^3 F_0 \tag{2.2}$$

almost everywhere, and appropriate boundary conditions at the endpoints of the interval. The simplest possibility is $\alpha = \alpha'' = 0$, which ensures smoothness, but at either endpoint it is also possible to introduce D6-branes (with $\alpha = 0$), O8-planes ($\alpha' = 0$), O6-planes ($\alpha'' = 0$).

NSNS flux quantization implies $N \in \mathbb{Z}$, while for RR it gives

$$-\frac{\alpha''(i)}{81\pi^2} \in \mathbb{Z}, \quad \forall i \in \mathbb{Z}. \tag{2.3}$$

$F_0 = \frac{n_0}{2\pi}$, $n_0 \in \mathbb{Z}$ is locally constant, but can jump across D8-branes; these are restricted to lie at integer values μ of z , which are in turn identified with their D6-brane charge. A cartoon of the internal geometry is shown in figure 1.

The curvature and string coupling of any given solution can be rescaled and made arbitrarily small by taking

$$N \gg 1 \quad \mu/N \text{ finite}. \tag{2.4}$$

This is the regime relevant for holography.

The simplest solution occurs when the Romans mass $F_0 = 0$. (2.2) implies that α'' is constant, and (2.3) implies

$$\alpha = \frac{81}{2}\pi^2 k z(N - z). \tag{2.5}$$

$k \in \mathbb{Z}$ is interpreted as the F_2 flux integer on the \mathbb{S}^2 . There are k D6-branes at $z = 0$ and $-k$ anti D6-branes at $z = N$. The resulting IIA solution is the dimensional reduction of the $\text{AdS}_7 \times \mathbb{S}^4/\mathbb{Z}_k$ solution of eleven-dimensional SUGRA.

When $F_0 \neq 0$, α'' is piecewise linear; it can be parameterized as

$$-\frac{\alpha''(z)}{81\pi^2} = r_i + (r_{i+1} - r_i)(z - i) \tag{2.6}$$

on each interval $z \in [i, i + 1]$. By eq. (2.3), the $r_i \in \mathbb{Z}$.

These AdS_7 solutions were conjectured to arise from the near-horizon limit of NS5-D6-D8 brane diagrams, and this led to the identification of the dual SCFT₆ [39]. We now give a quick review focused on what we need in this paper; see [14, section 2.1] for more details.

The brane diagram can be described as follows. There are N NS5-branes along directions 012345, separated along direction 5. Between the $(i - 1)^{\text{th}}$ and i^{th} NS5-brane, r_i D6-branes are suspended, along directions 0123456; crossing the latter, there are also $f_i = 2r_i - r_{i+1} - r_{i-1}$ D8-branes along 012345789. This brane diagram is depicted schematically in the black part of figure 2.

The six-dimensional field theory engineered by this diagram is a chain of $N - 1$ vector multiplets with gauge groups $U(r_i)$; there are hypermultiplets in each of the bifundamental representations $\overline{\mathbf{r}}_i \otimes \mathbf{r}_{i+1}$, and f_i in the fundamental \mathbf{r}_i . There are also $N - 1$ tensor multiplets.

(2.6) tells us that the function $r(z) \equiv -\alpha''/81\pi^2$ gives the ranks r_i when evaluated at $z = i$; conversely we can write

$$\alpha(z) = -81\pi^2 \frac{1}{\partial_z^2} r(z). \tag{2.7}$$

The integration constants in the double integral should be understood as being fixed by the boundary conditions. As an example, when $F = 0$ all the ranks are equal, $r_i = k$, and it is easy to see that eq. (2.7) reproduces eq. (2.5).

An important piece of evidence for the $\text{AdS}_7/\text{CFT}_6$ conjecture we just reviewed came from a holographic match of the a anomaly [14, 40]. At leading order in the limit eq. (2.4), the gravitational result reads

$$a_{6d,\text{hol}} = \frac{64}{189\pi^2} \int r \alpha dz = -\frac{192}{7} \int r \frac{1}{\partial_z^2} r dz. \tag{2.8}$$

In the second step we have used eq. (2.7). On the other hand, the leading term in the field theory computation is given by a Green-Schwarz term and reads

$$a_{6d} = \frac{192}{7} (C^{-1})^{ij} r_i r_j, \tag{2.9}$$

where C_{ij} is the Cartan matrix of A_{N-1} . C_{ij} is a discrete analogue of minus a double derivative: indeed

$$C_{ij} r_j = -r_{i+1} + 2r_i - r_{i-1} \sim -(\partial^2 r)_i \tag{2.10}$$

So its inverse is a discrete analogue of a double integral. Hence eq. (2.9) matches eq. (2.8) when $N \gg 1$.

To summarize the important lesson for our present purposes, in the holographic limit we have

$$\alpha^i = 81\pi^2(C^{-1})^{ij}r_j. \tag{2.11}$$

As an example, we can again look at the $F_0 = 0$ case, where $r_i = k$ and $(C^{-1})^{ij}r_j = \frac{1}{2}i(N-i)$, in agreement with eq. (2.5).

3 Probe brane holography

In this section, we construct embeddings for probe D4-branes in the asymptotically $\text{AdS}_7 \times M_3$ geometries reviewed in section 2 that are dual to BPS codimension-4 defects in six-dimensional $\mathcal{N} = (1, 0)$ SCFTs. Using these solutions for embedded AdS_3 branes, we characterize these defects by computing their independent defect Weyl anomalies using probe brane holography. First, we holographically compute the defect contribution to the EE of a spherical region in the dual field theory; this furnishes for us a specific linear combination of the two independent defect Weyl anomalies. Second, we compute the free energy of the defect wrapping $\mathbb{S}^2 \hookrightarrow \mathbb{R}^6$, which gives us the A-type defect anomaly a_Σ . The value of a_Σ matches the predicted value computed from in-flow, and so, bolsters the standing of the holographic prediction for the B-type anomaly d_2 . Lastly, compute the defect supersymmetry Casimir Energy (SCE), which is obtained holographically from the on-shell action of a probe brane wrapping $\mathbb{S}^1 \times \mathbb{S}^1 \hookrightarrow \mathbb{S}^1 \times \mathbb{S}^5$.

3.1 Probe D4-brane embedding

Throughout this section, we will work in Euclidean signature. The probe brane action is

$$S_{\text{probe}} = T_4 \int_{M_5} d^5x e^{-\phi} \sqrt{\det P[g + B]} + \mathcal{F} - T_4 \int_{M_5} e^{\mathcal{F}} \wedge P[C], \tag{3.1}$$

where

$$T_4 = \frac{1}{16\pi^4 l_s^5}; \tag{3.2}$$

M_5 is the D4-brane worldvolume with coordinates x^a , P denotes pull-back onto M_5 , and the worldvolume gauge field $\mathcal{F} = B + 2\pi l_s f$. Throughout, we will work with convention $l_s = 1$.

We will consider D4-brane probes of the factorized form

$$\widetilde{M}_3 \times \mathbb{S}^2 \subset \text{AdS}_7 \times M_3, \tag{3.3}$$

where $\widetilde{M}_3 \subset \text{AdS}_7$ and the \mathbb{S}^2 is the sphere appearing in eq. (2.1), whose z position we will determine shortly. Our D4-branes will carry non-zero D2-brane charge $j \in \mathbb{Z}$:

$$f = \frac{j}{2} \text{vol}_{\mathbb{S}^2}. \tag{3.4}$$

The position z of the D4 can be fixed by extremizing the action. This is implied by the BPS condition, which in general reads $\Gamma_{\parallel} \epsilon_2 = \epsilon_1$ for a D-brane, with Γ_{\parallel} the product of the parallel gamma matrices and ϵ_a the supersymmetry parameters preserved by the solution.

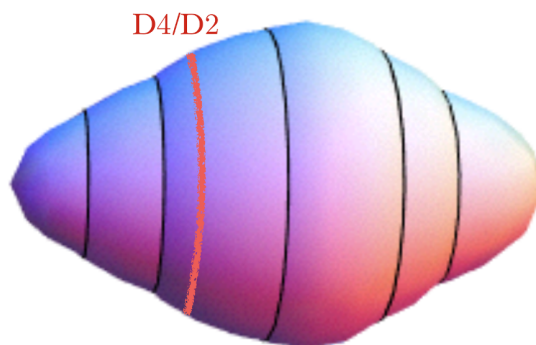


Figure 1. A cartoon of the internal three-dimensional space of the AdS₇ solution. The black creases represent the D8-branes, where the metric is continuous but not differentiable. The red locus represents a D4-D2 bound state probe, to be discussed in the next section.

In our case, the ϵ_a are factorized in terms of Killing spinors ζ in AdS₇ and internal spinors χ_a [12, (A.4)]. Γ_{\parallel} is also factorized because of our assumption (3.3).

The internal part $\gamma_{\parallel}\chi_1 = \chi_2$ of the BPS computation can be carried out efficiently in terms of calibrations. It is in fact identical to that for a D8/D6 bound state in [12, section 4.8], so we will be brief. (This happens because intersecting or overlapping D-branes preserve supersymmetry if the number of Neumann-Dirichlet directions is a multiple of 4.) The relevant condition is³

$$\mathcal{F} = \pi \frac{\alpha\alpha'}{\alpha'^2 - 2\alpha\alpha''} \text{vol}_{\mathbb{S}^2}. \tag{3.5}$$

Using (2.1), (3.4), this implies

$$z = j. \tag{3.6}$$

As anticipated, this coincides with the BPS position for a D8-brane with D6 charge equal to j , which was already noticed below (2.3).

The case of a single D2 has to be treated separately; again this works in the same way as a D6 extended along all of AdS₇. The calibration analysis this time gives $\alpha\alpha'' = 0$, which is only true at the extrema of the interval, $z = 0$ and $z = N$. The resulting probe D4-D2 bound state wraps an internal \mathbb{S}^2 at fixed $z = j$, which is schematically visualized in figures 1 and 2.

The probe brane action then takes the form

$$\begin{aligned} S_{\text{probe}} &= T_4 \int_{M_5} d^5x e^{3A-\phi} f_1^2 f_2 \sqrt{g_{\theta\theta} g_{\phi\phi} + \mathcal{F}_{\theta\phi}^2}|_{z=j} \tag{3.7} \\ &= \frac{64\pi}{81} T_4 \text{vol}(\widetilde{M}_3) \sqrt{\alpha'^2 - \alpha\alpha''} \left(\left(\sqrt{-\frac{\alpha''}{\alpha}} \frac{\sqrt{2}\alpha^2}{\alpha'^2 - 2\alpha\alpha''} \right)^2 + \left(\frac{\alpha\alpha'}{\alpha'^2 - 2\alpha\alpha''} \right)^2 \right)^{1/2} \\ &= \frac{64\pi}{81} T_4 \text{vol}(\widetilde{M}_3) \alpha^j, \end{aligned}$$

³In the language of [12], the calibration is $\text{Im}\psi_+^1$; alternatively, one can impose that the forms $(\text{Im}\psi_+^2, \text{Re}\psi_+^2, \text{Re}\psi_+^1)$ pull back to zero.

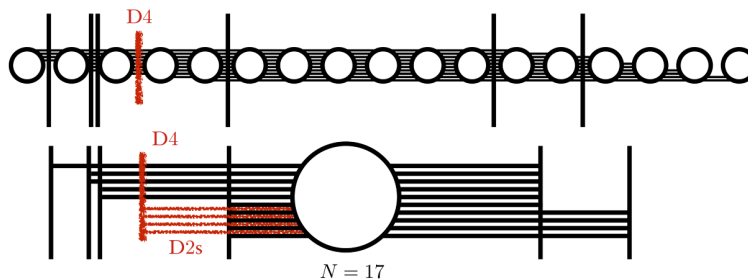


Figure 2. The black part is a schematic representation of the NS5-D6-D8 brane diagram, taken from [14]. The nodes, horizontal lines and vertical lines represent NS5-, D6- and D8-branes respectively. The upper part of the diagram, where the NS5 are separated, is more useful to read the field theory. The red vertical lines here represent additional D4-branes, which engineer line defects in the field theory, to be discussed in the next section. The lower part, where the NS5-branes coincide, corresponds to the conformal phase of the field theory, and resembles more directly the gravity solution. The brane-creation effect changes the number of D6-branes, and leads to the creation of D2-branes, represented by red horizontal lines. In the near-horizon limit, each D8 with D6s ending on it becomes a D8-D6 bound state, and the D4 with D2s becomes a D4-D2 bound state.

where we introduced $\alpha^j \equiv \alpha(j)$. In the second line, we have used (2.1). Since the D2 charge carried by the probe D4 brane eliminated the explicit z dependence, the action completely factorized into a product of an integral over the volume form of the \widetilde{M}_3 and an integral over the internal S^2 geometry threaded by two-form flux.

In what follows we will consider a more general situation where there is a collection of q_j D4-branes with D2-brane equal to j . This will turn (3.7) into $\frac{64\pi}{81} T_4 \text{vol}(\widetilde{M}_3) q_j \alpha^j$. We will work in the probe approximation: this requires $q_j e^{\phi(j)} \ll 1$, which by (2.1) is implied by $q_j \ll \sqrt{N}$.

It is clear from the form of the on-shell action in eq. (3.7) that we will need to regulate divergences coming from $\text{vol}(\widetilde{M}_3)$. To that end, we will use the holographic renormalization scheme for probe branes developed in [41]. As a brief review, this is done by introducing a large radial cutoff Λ in the background AdS_7 geometry and computing the covariant counterterms on the intersection of the radial hypersurface and the worldvolume of the probe brane. We denote coordinates on this intersection by y^a and the induced metric by γ_Λ . Since, we have no worldvolume scalars turned on in our embedding, the only counterterm that we need to compute is the volume of the intersection

$$S_{\text{CT}} = -\frac{2\pi}{9} T_4 \sqrt{2r_j \alpha^j} \int d^2 y \sqrt{\gamma_\Lambda}, \tag{3.8}$$

where the coefficient is fixed to cancel polynomial divergences in Λ appearing in $\text{vol}(\widetilde{M}_3)$. In the subsections below, we denote the holographically renormalized probe brane action by

$$S_{\text{ren}} = S_{\text{probe}} + S_{\text{CT}}. \tag{3.9}$$

3.2 Spherical entanglement entropy

Here we compute the contribution of the probe string defect to the spherical entanglement entropy (EE). For simplicity, we will consider a flat embedding of a two-dimensional defect supported on $\mathbb{R}^{1,1}$ in $\mathbb{R}^{5,1}$, which will be taken as the conformal boundary of the AdS_7 part

of the background solution. Since we are working entirely within the probe limit, we do not need to compute the backreaction and can compute the EE by using [42].

First, we consider the AdS₇ part of the background geometry in flat slicing

$$ds_7^2 = \frac{1}{u^2}(du^2 - dt^2 + dx_1^2 + d\xi^2 + \xi^2 d\Omega_3^2), \quad (3.10)$$

with the probe D4-brane wrapping $\{t, x_1, u\}$ and $d\Omega_3^2$ the line element on the unit S^3 . Following [42, 43], we map

$$\begin{aligned} t &= \frac{R\sqrt{\rho^2 - 1} \sinh \tau}{\rho \cosh v + \sqrt{\rho^2 - 1} \cosh \tau}, & u &= \frac{R}{\rho \cosh v + \sqrt{\rho^2 - 1} \cosh \tau}, \\ x_1 &= \frac{R\rho \sinh v \cos \phi}{\rho \cosh v + \sqrt{\rho^2 - 1} \cosh \tau}, & \xi &= \frac{R\rho \sinh v \sin \phi}{\rho \cosh v + \sqrt{\rho^2 - 1} \cosh \tau}, \end{aligned} \quad (3.11)$$

which after a Wick rotation brings us to the seven-dimensional hyperbolic black hole [42]

$$ds_7^2 = \frac{d\rho^2}{f(\rho)} + f(\rho)d\tau^2 + \rho^2 dv^2 + \rho^2 \sinh^2 v (d\phi^2 + \sin^2 \phi d\Omega_3^2) \quad (3.12)$$

where the metric function

$$f(\rho) = \rho^2 - 1, \quad (3.13)$$

and $\tau \sim \tau + 2\pi$. The BPS probe brane embedding found in section 3.1 now wraps $\{\tau, v, \rho\}$. The probe brane contributions to the thermal entropy in the hyperbolic black hole background corresponds to the holographic computation of the BPS surface defect contribution to the EE of a spherical region in the dual field theory.

More generally, one can consider (not necessarily BPS) probe brane embeddings in seven-dimensional black hole solutions with metric function

$$f(\rho) = \rho^2 - 1 - \frac{\rho_h^4}{\rho^4}(\rho_h^2 - 1) \quad (3.14)$$

with the location of the horizon determined in terms of the inverse temperature β by

$$\rho_h = \frac{1}{3\beta} \left(\pi + \sqrt{\pi^2 + 6\beta^2} \right). \quad (3.15)$$

This background is particularly useful for the holographic computation of Rényi entropies [44]. Moving to a branched cover of the black hole geometry $\tau \sim \tau + \beta$ with $\beta = 2\pi n$, the thermal entropy in this background is dual to the n^{th} -Rényi entropy

$$S^{(n)} = \frac{2\pi n}{1-n} (\mathcal{F}(2\pi) - \mathcal{F}(2\pi n)), \quad (3.16)$$

where $\mathcal{F}(\beta) = \beta^{-1} S_{\text{ren}}(\beta)$. Clearly from the bulk geometry, the limit $n \rightarrow 1$ recovers the seven-dimensional hyperbolic black hole background, and in the dual field theory $S^{(n)}|_{n \rightarrow 1} \rightarrow S_{\text{EE}}$ [43, 44], which holographically

$$S_{\text{EE}} = \beta^2 \partial_\beta (\beta^{-1} S_{\text{ren}}(\beta))|_{\beta \rightarrow 2\pi}. \quad (3.17)$$

Computing the holographic renormalized on-shell action, we begin with

$$\text{vol}(\widetilde{M}_3) = \int_0^\beta d\tau \int_0^{v_c} dv \int_{\rho_h}^\Lambda \rho d\rho = \frac{\beta}{2} v_c (\Lambda^2 - \rho_h^2), \quad (3.18)$$

where we have introduced a large radial cutoff Λ . The Λ^2 divergence is regulated by eq. (3.8)

$$S_{\text{CT}} = -\frac{32\pi}{81} \beta T_4 v_c \Lambda^2 \rho_h^2 \alpha^j. \quad (3.19)$$

Using eq. (3.11), the linear divergence in v_c in the black hole background is related to a log divergence at small $u = -\epsilon$

$$v_c = \log \frac{2R}{\epsilon}, \quad (3.20)$$

where R is the radius of the boundary spherical entangling surface that anchors the homologous Ryu-Takayanagi surface [45] in the bulk. Thus, we find that the near boundary behavior of the holographically renormalized action is⁴

$$S_{\text{ren}} = -\frac{8}{81} q_j \alpha^j T_4 \text{vol}(\mathbb{S}^2) \beta \rho_h^2 \log \frac{2R}{\epsilon} + \dots \quad (3.21)$$

Using the form of ρ_h in eq. (3.15), we find the defect sphere EE is

$$S_{\text{EE}} = \frac{8}{405\pi^2} q_j \alpha^j \log \frac{2R}{\epsilon} + \dots \quad (3.22)$$

In the $F_0 = 0$ case, we can evaluate the previous quantities more explicitly using eq. (2.5). For example eq. (3.22) becomes

$$S_{\text{EE}} = \frac{4k}{5} \sum_j q_j j (N - j) \log \frac{2R}{\epsilon} + \dots \quad (3.23)$$

From [27, 34], we know that for a flat two-dimensional conformal defect embedded in a CFT on a flat six-dimensional background the universal part of the defect sphere EE is uniquely determined by defect Weyl anomalies:

$$S_{\text{EE}} = \frac{1}{3} \left(a_\Sigma - \frac{3}{5} d_2 \right) \log \frac{2R}{\epsilon} \quad (3.24)$$

Further, we know that for a two-dimensional superconformal preserving at least $\mathcal{N} = (2, 0)$ defect supersymmetry, the two B-type defect Weyl anomaly coefficients, d_1 and d_2 , are equal [32, 33], and so the universal part of the defect sphere EE, when combined with an independent computation of either a_Σ or d_2 , provides some measure of characterization of the defect degrees of freedom via anomalies. In the next subsection, we will compute the on-shell action for probe branes wrapping \mathbb{S}^2 and $\mathbb{S}^1 \times \mathbb{S}^1$ in the boundary geometry, which will give us independent predictions for a_Σ and d_2 .

⁴For $\beta \neq 2\pi$, the defect embedding is expected to get deformed; this deformation is not known analytically and would not be BPS. However, we are evaluating the action, which on shell is stationary under small deformations; so $\partial_\beta S_{\text{ren}}(\beta)|_{\beta \rightarrow 2\pi} = 0$, and we can use directly the expression (3.21) in (3.17) [46, 47].

In addition to the defect sphere EE, which can be found by taking $n \rightarrow 1$ in eq. (3.16), there are other limits of $S^{(n)}$ that contain interesting physical information (see e.g. [44]). By setting $\beta = 2\pi n$ and computing the renormalized on-shell action, we find that the n^{th} Rényi entropy is

$$S^{(n)} = T_4 q_j \alpha^j \text{vol}(\mathbb{S}^2) \text{vol}(\widetilde{\mathbb{S}}^2) \log \frac{2R^2 \left(1 - 6n^2 + \sqrt{1 + 24n^2}\right)}{\epsilon \cdot 729n(1-n)} + \dots \quad (3.25)$$

Taking the $n \rightarrow 0$ limit counts the number of non-zero eigenvalues of the reduced density matrix:

$$\lim_{n \rightarrow 0} S^{(n)} = \frac{4}{729n\pi^2} q_j \alpha^j \log \frac{2R}{\epsilon} + O(n^0). \quad (3.26)$$

Taking the opposite limit, $n \rightarrow \infty$, measures the largest eigenvalue of the reduced density matrix

$$\lim_{n \rightarrow \infty} S^{(n)} = \frac{4}{243\pi^2} q_j \alpha^j \log \frac{2R}{\epsilon} + O(n^{-1}). \quad (3.27)$$

3.3 On-shell action

In this subsection, we compute the holographically renormalized on-shell action in eq. (3.9) starting from eq. (3.7) for the cases where the boundary geometry of \widetilde{M}_3 is \mathbb{R}^2 , \mathbb{S}^2 , and $\mathbb{S}^1 \times \mathbb{S}^1$. In the latter two cases, the computations result in robust predictions for physical quantities that will be compared to anomaly inflow and supersymmetric localization at large N in the following sections.

3.3.1 \mathbb{R}^2

Here we compute the on-shell action for a probe D4-brane embedding into eq. (2.1) wrapping $\text{AdS}_3 \times \mathbb{S}^2$ engineering a flat two-dimensional defect supported on \mathbb{R}^2 in the dual field theory defined on a \mathbb{R}^6 background. We take the AdS_7 to be written in flat slicing as in eq. (3.10). We fix static gauge with $\xi = 0$ such that the full $\text{SO}(4)_N$ normal bundle symmetry is preserved. Computing the pullback onto the worldvolume of the probe D4-branes, the induced metric takes the form

$$\frac{ds_{\Sigma}^2}{\pi\sqrt{2}} = f_1^2(dx_0^2 + dx_1^2) + f_2^2 du^2 + f_3^2 d\Omega_2^2. \quad (3.28)$$

Computing the on-shell action eq. (3.7), only finding $\text{vol}(\widetilde{M}_3)$ remains to be done. For the embedding described above,

$$\text{vol}(\widetilde{M}_3) = \text{vol}(\mathbb{R}^2) \int_{-\infty}^{-\epsilon} \frac{du}{u^3} = \frac{\text{vol}(\mathbb{R}^2)}{2\epsilon^2}, \quad (3.29)$$

where we have introduced a small radial cutoff $u = -\epsilon$. There are no subleading divergences, and so the covariant counterterm action built out of the induced volume of the cutoff slice $u = -\epsilon$ exactly cancels S_{probe} leaving

$$S_{\text{ren}} = 0, \quad (3.30)$$

as expected.

3.3.2 \mathbb{S}^2

Since we are studying a particularly simple D4-D2 bound state system as a probe, we can easily consider other AdS₇ and AdS₃ geometries that will reveal the anomaly. Instead of using flat slicing in Poincaré coordinates, we can consider the background AdS₇ geometry in global coordinates with radial slices having $\mathbb{H}^5 \times \mathbb{S}^1$ geometry using the map in appendix A, which results in

$$ds_7^2 = d\sigma^2 + \cosh^2 \sigma ds_{\mathbb{H}_5}^2 + \sinh^2 \sigma d\varphi^2, \quad (3.31)$$

where the line element on the \mathbb{H}_5 is given in eq. (A.8). So (3.31) is essentially (3.12), but with the defect now wrapping an equatorial $\mathbb{S}^2 \hookrightarrow \mathbb{S}^4 \subset \mathbb{H}_5$. Thus, our D4-D2 bound state probe can be embedded in such a way that it wraps the boundary submanifold $\psi = \pi/2$ at the boundary $\rho \rightarrow \infty$ at fixed σ .

Computing the on-shell action in this background is straightforward:

$$S_{\text{probe}} = \frac{16}{81} T_4 (4\pi)^2 \alpha^j \int_0^{\log \Lambda} d\rho \sinh^2 \rho = \frac{32\pi^2}{81} T_4 \alpha^j \left(\Lambda^2 - 4 \log \Lambda + \dots \right). \quad (3.32)$$

We have introduced a radial cutoff $\rho = \log \Lambda \gg 1$ and suppressed further subleading (finite) terms. Note that in this curved space embedding, $z = j$ still extremizes the action, and so we can use this to evaluate the action on-shell. The counterterm action is computed from (3.8). We can tune c_1 to remove the Λ^2 divergence, and so the holographically renormalized on-shell action is

$$S_{\text{ren}} = -\frac{8}{81\pi^2} q_j \alpha^j \log \Lambda. \quad (3.33)$$

This log divergence is physical: it holographically computes the A-type Weyl anomaly for a defect wrapping \mathbb{S}^2 inserted into the six-dimensional $\mathcal{N} = (1, 0)$ SCFT dual to the ten-dimensional SUGRA solution above:

$$\langle \mathcal{O}_{\mathbb{S}^2} \rangle \approx e^{-S_{\text{ren}}} = (R\mu)^{a_\Sigma/3} \quad (3.34)$$

where we have introduced the length scale R on the \mathbb{S}^2 along with the RG scale μ for dimensional reasons. Equating

$$S_{\text{ren}} = -\frac{1}{3} a_\Sigma \log \Lambda \quad (3.35)$$

and using (3.33), we find a prediction for the A-type defect Weyl anomaly to leading order in large N :

$$a_\Sigma = \frac{8}{27\pi^2} q_j \alpha^j. \quad (3.36)$$

In order to compute the B-type anomaly, we insert (3.36) into (3.24) and use (3.22) to arrive at

$$d_1 = d_2 = \frac{32}{81\pi^2} q_j \alpha^j. \quad (3.37)$$

We can express a_Σ in terms of representation theoretic data, like for the Wilson surface in the $(2, 0)$ theory [27, 48]. Recalling eq. (2.11), we can rewrite

$$a_\Sigma = 24q_i(C^{-1})^{ij}r_j = 24(q, r), \quad d_1 = d_2 = 32(q, r), \quad (3.38)$$

where we defined the Killing form on the weight space:

$$(\lambda, \lambda') \equiv \lambda_i(C^{-1})^{ij}\lambda'_j. \quad (3.39)$$

As a simple example, consider the case where $F_0 = 0$. All the $r_i = k$, so $r = k\rho_W$, where $\rho_W = (1, 1, \dots, 1)$ is the Dynkin label for the A_{N-1} Weyl vector. Moreover take a single probe brane in position j : $q_j = 1$, $q_{i \neq j} = 0$. We obtain

$$a_\Sigma = 12k \sum_j j(N-j) = 24k(\lambda, \rho_W) = \frac{3}{4}d_2 \quad (3.40)$$

where now

$$\lambda = (\underbrace{0, \dots, 0}_{j-1}, 1, \underbrace{0, \dots, 0}_{N-j-1}). \quad (3.41)$$

3.3.3 $\mathbb{S}^1 \times \mathbb{S}^1$

Even though we already have the two independent defect Weyl anomalies in hand, there are other defect geometries whose partition function carry non-trivial information related to anomalies. Here we consider the probe brane geometry dual to the Wilson surface operator wrapping $\mathbb{S}_{R_6}^1 \times \mathbb{S}^1 \hookrightarrow \mathbb{S}_{R_6}^1 \times \mathbb{S}^5$. The purpose of computing the on-shell action for this probe brane configuration is two-fold. First, upon dimensional reduction along $\mathbb{S}_{R_6}^1$, the BPS Wilson surface operator descends to the circular Wilson loop W in $\mathcal{N} = 1$ SYM theory on \mathbb{S}^5 . This opens up the possibility of comparing to exact results for $\langle W \rangle$ obtained in the field theory using supersymmetric localization. Second, the partition function Z of an SCFT on $\mathbb{S}_\beta^1 \times \mathbb{S}^{d-1}$ has long been known to be related to the superconformal index \mathcal{I} up to an exponential pre-factor containing a term known as the supersymmetric Casimir Energy (SCE), $Z = e^{-\beta E_c} \mathcal{I}$ that can be computed in terms of various anomalies [49–51]. In the case of a superconformal field theory, the defect SCE can be related to Weyl anomalies and in the case of superconformal defects, has been computed in several cases [52]. However, it only has been rigorously proven to be related to defect anomalies for co-dimension four defects in six dimensional $\mathcal{N} = (2, 0)$ SCFTs [53].

Returning the probe brane computation, the coordinate transformation to take us to a probe brane wrapping $\mathbb{S}^1 \times \mathbb{S}^1$ is discussed in appendix A ending with the AdS₇ metric in eq. (A.16). We then take the periodicity around the $\mathbb{S}_{R_6}^1$ to be $\tau \sim \tau + 2\pi R_6$. On the field theory side in the dimensional reduction along $\mathbb{S}_{R_6}^1$ to a Wilson loop wrapping a great circle on \mathbb{S}^5 , the five-dimensional Yang-Mills coupling is related to the radius of the compactified direction by

$$R_6 = \frac{g_{\text{YM}}^2}{8\pi^2}. \quad (3.42)$$

Integrating over the \mathbb{S}^2 and the \mathbb{S}^1 s wrapped in the boundary geometry, the on-shell action takes the form

$$S_{\text{probe}} = \frac{128\pi^3 R_6}{81} T_4 q_j \alpha^j \int_0^{\log \Lambda} d\sigma \sinh 2\sigma = -\frac{64\pi^3 R_6}{81} T_4 q_j \alpha^j \left(\frac{\Lambda^2}{2} - 1 + \frac{1}{2\Lambda^2} + \dots \right) \quad (3.43)$$

Again using eq. (3.8) as the counterterm action, the Λ^2 divergence is regulated, and we find the holographically renormalized on-shell action

$$S_{\text{ren}} = -\frac{64\pi^3 R_6}{81} T_4 q_j \alpha^j. \quad (3.44)$$

In order to more easily compare to the field theory computation, we define $\beta = 4\pi R_6$, hence

$$\langle W \rangle = \exp \left[\frac{\beta}{81\pi^2} q_j \alpha^j \right] = \exp \left[\beta q_i (C^{-1})^{ij} r_j \right], \quad (3.45)$$

which in the $F_0 = 0$ case gives

$$\langle W \rangle = \exp \left[\frac{\beta}{2} k \sum_j q_j j (N - j) \right]. \quad (3.46)$$

In the following section, we will compare eq. (3.46) to the field theory calculation of the expectation value of a circular Wilson loop in five-dimensional SYM theory on \mathbb{S}^5 computed using supersymmetric localization.

Due to the nature of the holographic computation, it should not be entirely surprising that $\langle W \rangle$ can be expressed in a form similar to the defect Weyl anomalies. However, without detailed knowledge of how the defect SCE of surface operators in six-dimensional $\mathcal{N} = (1, 0)$ SCFTs should be related to defect Weyl anomalies, we cannot say what linear combination of a_Σ and d_2 should be computed by $\langle W \rangle$. In the case of a Wilson surface in the six-dimensional A_{N-1} $\mathcal{N} = (2, 0)$ theory, however, it has been shown using chiral algebra methods that d_2 alone appears in the defect SCE [53], which leads to the conjecture that the relation to the defect Weyl anomalies in eq. (3.46) is not just superficial and that at large N the defect SCE is given by $E_c = d_2/32$, though a proof is lacking.

3.4 Defect gravitational anomaly

Here, we compute the defect gravitational anomaly from the worldvolume action of the probe brane in the $\text{AdS}_7 \times M_3$ geometry in eq. (2.1). In the anomaly polynomial this is the coefficient of the first Pontryagin class of the defect submanifold Σ :

$$\mathcal{I}_4 = \frac{k_r}{2} c_1(r) - \frac{k_g}{24} p_1(T). \quad (3.47)$$

$p_1(T\Sigma) = \frac{\text{Tr}(R_T \wedge R_T)}{8\pi^2}$ is related by descent mechanism to the gravitational three-dimensional Chern-Simons form,

$$p_1 = 2\pi d\text{CS}_3(R_T) \quad \text{CS}_3(R_T) = \frac{1}{4\pi} \text{tr} \left(\Gamma_T \wedge d\Gamma_T + \frac{2}{3} \Gamma_T^3 \right), \quad (3.48)$$

where $R_T^a{}_b = (d\Gamma_T + \Gamma_T^2)^a{}_b = \frac{1}{2}R^a{}_{b\mu\nu}dx^\mu \wedge dx^\nu$ is the curvature of Σ . Explicitly we have

$$\text{tr}(R_T \wedge R_T) = \frac{1}{4}R^a{}_{b\rho\sigma}R^b{}_{a\mu\nu}dx^\mu \wedge dx^\nu \wedge dx^\rho \wedge dx^\sigma \quad (3.49)$$

The anomaly appears in the partition function as a phase,

$$e^{2\pi i\mathcal{A}} = e^{ik_g \int_{M_3} \frac{\text{CS}_3(R_T)}{24}} \quad (3.50)$$

where for us M_3 will be AdS_3 .

In order to evaluate the gravitational anomaly, we apply the strategy adopted in [54]. To start, we need to look at the worldvolume action of a stack of q_i D4-branes wrapping $\mathbb{S}_{z=i}^2 \subset M_3$ and extending along AdS_3 . In particular we focus on the Wess-Zumino term that includes the gravitational contribution,

$$S_{\text{D4}}^{\text{WZ}} = T_4 \int_{M_8} \text{Tr} \left[\sum_n C_n \wedge e^{\mathcal{F}} \wedge \sqrt{\widehat{A}(2\pi R_T)} \right]_5, \quad (3.51)$$

where the A-roof genus reads

$$\widehat{A}(R) = 1 - \frac{1}{24}p_1(T\Sigma) + \dots \quad (3.52)$$

If we ignore the term due to the non-abelian scalars, the term proportional to $p_1(T\Sigma)$ reads

$$S_{\text{D4}}^{\text{WZ}} \supset -q_i \int_{M_5} (C_1 - C_{-1}B_2) \wedge \frac{1}{24}p_1(T\Sigma), \quad (3.53)$$

where q_i comes from the trace of the identity matrix. In addition we also accounted for the IIA Romans mass contribution F_0 which formally can be written as $F_0 = dC_{-1}$. Integrating by parts and by using (3.51), we obtain

$$S_{\text{D4}}^{\text{WZ}} \supset -q_i \int_{\mathbb{S}_{z=i}^2} (F_2 - F_0 B_2) \int_{\text{AdS}_3} \frac{\text{CS}_3(R_T)}{24 \times 2\pi}. \quad (3.54)$$

By inputting the eq. (2.1) and by integrating over $\mathbb{S}_{z=i}^2$ we get

$$S_{\text{D4}}^{\text{WZ}} \supset -q_i r_i \int_{\text{AdS}_3} \frac{\text{CS}_3(R_T)}{24}. \quad (3.55)$$

We now have to compare this result with the argument in (3.50). Considering multiple stacks of D4-branes, we obtain the gravitational anomaly

$$k_g = - \sum_i q_i r_i. \quad (3.56)$$

This matches the field theory computation in eq. (B.18).

Let us now briefly comment on the computation that led to eq. (3.55) with an eye toward section 4.2. First, notice that the defect gravitational anomaly is not directly captured by inflow. Further, it does not have the same product structure of the bulk-defect degrees of freedom, where the metric of the string lattice and its dual appear. A possible interpretation

for this is that the gravitational anomaly accounts for the modes living only on the defect and not interacting with the bulk six-dimensional SCFT. The latter does not capture the inflow contribution, but it reproduces the gravitational anomaly computation that we just performed in gravity purely from field theory. Finally we speculate that the gravitational anomaly computation provides the only contribution to the subleading correction of the defect a_Σ anomaly in the large r_i and N limit. In other words, the on-shell action provides the leading contribution, whereas the WZ action gives the subleading one. This would work exactly like in [54]. The total a_Σ anomaly would then read [30]

$$a_\Sigma = 3k_r - \frac{k_g}{2} = 24q_i(C^{-1})^{ij}r_j + \frac{\sum_i q_i r_i}{2}. \tag{3.57}$$

4 Anomalies from field theory and their string theory constructions

In this section, we test the holographic predictions provided by the probe brane computations in the previous section in two different settings. In the first subsection, we employ supersymmetric localization to compute the expectation value of a circular Wilson loop operator inserted in the antisymmetric representation of a necklace quiver gauge theory on S^5 . This Wilson loop operator is thought to have UV completion to the string defect operator studied in section 3.3.3, and so we compare the localization computation to the holographic result for $\langle W \rangle$. In the second subsection, we take a different approach. We first rely on IIB/F-theory constructions of the 6d $\mathcal{N} = (1, 0)$ SCFTs to compute defect anomalies using inflow arguments. We then use known non-perturbative relations between 't Hooft anomalies and the A-type Weyl anomaly for superconformal two-dimensional defects to compute a_Σ . In both cases, we find exact agreement with the probe brane results.

4.1 Necklace quivers and supersymmetry localization on S^5

In this section, we demonstrate that the holographically renormalized on-shell action in eq. (3.44) can be matched with the expectation value of the Wilson loop in the five-dimensional $\mathcal{N} = 1$ theory described by a circular quiver with k $SU(N)$ gauge groups and the massless bifundamental hypermultiplet between the two gauge groups that are next to each other. This quiver theory can be regarded as a Kaluza-Klein (KK) theory whose UV completion is the six-dimensional $\mathcal{N} = (1, 0)$ theory living on N M5-branes on the $\mathbb{C}^2/\mathbb{Z}_k$ singularity (see e.g. [55, section 4]).

Just like in section 2, this six-dimensional $\mathcal{N} = (1, 0)$ theory can be realized using the Type IIA brane system consisting of k D6-branes in the 0123456 directions, along with N NS5-branes in the 012345 directions; unlike in the general case, no D8-branes are necessary. The defect is regarded as a D4-brane spanning the 01789 directions and is located between the $(j - 1)$ -th and j -th NS5-branes. The distance between such two NS5-branes gives rise to a tension of a BPS string which is represented by the D2-brane in the 016 direction. A D6-brane observer sees the D2 brane as a gauge instanton. The 2-4 and 4-2 strings stretched between the D2-branes and D4-branes give rise to fermionic fields in the D2-brane worldvolume. This is, in fact, precisely the T-dual of the D5-brane Wilson loops on the D3-brane worldvolume studied in [56, section 4.1] (see also [57]). As pointed out in those references, this brane system realizes the Wilson loop in 4d $\mathcal{N} = 4$ super-Yang-Mills theory

in the rank- s antisymmetric representation. The latter can be seen by integrating out the fermions associated with the 3-5 and 5-3 strings, where s is the fundamental string charge carried by the D5-brane. This argument therefore leads us to consider the Wilson loop in the rank- j antisymmetric representation of each gauge group in the circular quiver. In particular, we will show that the expectation value of the Wilson loop in question is related to the Weyl anomalies of the D4-brane defects in such a brane configuration.

The expectation value of the Wilson loop in the rank- j antisymmetric representation \wedge^j of five-dimensional $\mathcal{N} = 1$ SYM with $SU(N)$ gauge group was performed in [21, section 2.3]:

$$\langle W_{\wedge^j} \rangle = \exp\left(\frac{\beta}{2}j(N-j)\right), \quad \beta \equiv \frac{g_{\text{YM}}^2}{2\pi r} \quad (4.1)$$

where r is the radius of the five-sphere which the Wilson loop wraps. On the other hand, the authors of [58, 59] also considered the circular quiver as described above, where the Wilson loop was taken to be in the fundamental representation \mathbf{N} of *one* of the $SU(N)$ gauge groups and in the trivial representation $\mathbf{1}$ of the others. They found that its expectation value turns out to be equal to eq. (4.1) with $j = 1$, namely that of the Wilson loop in the fundamental representation of the five-dimensional $\mathcal{N} = 1$ SYM with $SU(N)$ gauge group [58, 60]:

$$\langle W_{(\mathbf{N}, \mathbf{1}, \dots, \mathbf{1})} \rangle = \exp\left(\frac{\beta}{2}(N-1)\right) \stackrel{N \rightarrow \infty}{\sim} \exp\left(\frac{\beta}{2}N\right), \quad (4.2)$$

where the gauge coupling of each gauge group in the circular is taken to be equal to g_{YM} . Our main goal is to generalize these results, namely to compute the expectation value $\langle W_{(\wedge^j, \wedge^j, \dots, \wedge^j)} \rangle$ of the Wilson loop in the rank- j antisymmetric representation of every $SU(N)$ gauge group in the circular quiver.

To achieve this, we proceed as in [58, section 4.3], [59, section 3] and [21, section 2]. According to [59, (3.22)], the eigenvalue distribution of each $SU(N)$ gauge group in the circular quiver can be taken to be the same. We denote these by ϕ_i , with $i = 1, \dots, N$. The expression of the partition function then simplifies, whereby in the large N limit it takes the form

$$Z \sim \int \prod_{i=1}^N d\phi_i \exp\left[-k\frac{N^2}{\beta} \sum_{i=1}^N \phi_i^2 + k\frac{N}{2} \sum_{1 \leq i \neq l \leq N} |\phi_i - \phi_l|\right] \quad (4.3)$$

which is indeed a simple modification of the matrix model associated with five-dimensional $\mathcal{N} = 2$ SYM given by [21, (2.3)]. The latter can simply be obtained from eq. (4.3) by setting $k = 1$. The saddle points are the same as in [21, (2.4), (2.5)]:

$$0 = -\frac{2N^2}{\beta}\phi_i + N \sum_{l, l \neq i} \text{sign}(\phi_i - \phi_l); \quad (4.4)$$

$$\phi_i = \frac{\beta}{2N}(N - 2i), \quad \text{for } \phi_i > \phi_l \text{ whenever } i < l. \quad (4.5)$$

Note that, upon evaluating the exponential function in the integrand of eq. (4.3) at the saddle points, we find that the free energy $F = -\log Z$ obtained from above is indeed k times that of the five-dimensional $\mathcal{N} = 2$ SYM with $SU(N)$ gauge group, as pointed out in [61,

(3.11)], [58, (4.30)], and [59, section 4.3]. Let us now proceed with the computation of the Wilson loop expectation value. Similarly to [21, (2.15)], this is given by

$$\langle W_{(\wedge^j, \wedge^j, \dots, \wedge^j)} \rangle \sim \int \prod_{i=1}^N d\phi_i \exp \left[-k \frac{N^2}{\beta} \sum_{i=1}^N \phi_i^2 + k \frac{N}{2} \sum_{1 \leq i \neq l \leq N} |\phi_i - \phi_l| + kN \sum_{i=1}^j \phi_i \right]. \quad (4.6)$$

Since the derivative with respect to ϕ_i of the last term in the exponential gives a constant kN for all $i = 1, \dots, j$, the insertion of the Wilson loop does not change the eigenvalue distribution. Evaluating the exponential function containing the last term yields

$$\langle W_{(\wedge^j, \wedge^j, \dots, \wedge^j)} \rangle \sim \exp \left(kN \sum_{i=1}^j \phi_i \right) \Big|_{(4.5)} \sim \exp \left(\frac{\beta}{2} kj(N-j) \right). \quad (4.7)$$

The argument of the exponential function is in agreement with the holographic prediction for the surface operator wrapping $\mathbb{S}^1 \times \mathbb{S}^1$ with vanishing Romans mass in eq. (3.46) for a single defect $q_j = 1$.

4.2 Anomaly inflow from type IIB

In this subsection, we derive the a_Σ anomaly on the defect via inflow mechanism from the F-theory construction of six-dimensional $\mathcal{N} = (1, 0)$ SCFTs [10, 55, 62]. These backgrounds can be described in terms of type IIB string theory on a complex two-dimensional space with a non-trivial fibration of the axio-dilaton. When the space is singular, IIB on the singularity engineers the SCFT. If instead the space is resolved, which then denote by \mathcal{B} , IIB provides a definition of the tensor branch effective field theory (EFT) and corresponds to the scalars in the tensor multiplets acquiring non-trivial vacuum expectation values. The full BPS physics of the tensor branch EFT is determined by the geometric structure of the 2-cycles in \mathcal{B} which read

$$\begin{aligned} \int_{\mathcal{B}} \beta_i \wedge \beta_j &= A_i \cdot A_j = \int_{A_i} \beta_j = \Omega_{ij} \\ \int_{\mathcal{B}} \beta_i \wedge \alpha^j &= A_i \cdot B^j = \int_{B^j} \beta_i = \delta_i^j. \end{aligned} \quad (4.8)$$

Here \cdot denotes the number of intersections between cycles, weighted by signs so as to be topologically invariant; $\beta_i, \alpha^i, B^i, A_i$ generate the compact and non-compact cohomology and homology:

$$\begin{aligned} \beta_i &\in H_c^2(\mathcal{B}), & \alpha^i &\in H_{\text{nc}}^2(\mathcal{B}) \\ B^i &\in H_2^{\text{nc}}(\mathcal{B}), & A_i &\in H_2^c(\mathcal{B}). \end{aligned} \quad (4.9)$$

The axio-dilaton depends on the coordinates of the base and it is interpreted as the complex structure of a \mathbb{T}^2 fibered over \mathcal{B} . Crucially, the axio-dilaton degenerates over some loci of \mathcal{B} , and the type of monodromy around these singular loci determines which D7-branes spans the singular loci. Since we want to have supersymmetric configurations, the singular loci themselves are the holomorphic 2-cycles of \mathcal{B} . In addition, we associate a gauge algebra to a given D7-brane, which can be trivial or non-trivial or even of exceptional type. The RR four-form potential of type IIB is expanded as

$$C_4 = B_2^i \wedge \beta_i \quad (4.10)$$

providing the dynamical anti-symmetric two-form fields B_2^i . The bosonic content of the tensor multiplet is then completed by the real scalar modulus corresponding to

$$\text{Vol}(A_i) = \int_{A_i} J = \Omega_{ij} \phi^j, \quad J = \phi^i \beta_i, \quad (4.11)$$

where J is the Kähler form of \mathcal{B} . Lastly, we have D3-branes wrapping A_i , which are electrically charged under C_4 and therefore under the tensor multiplets. They form a lattice of BPS strings whose pairing is given by Ω_{ij} .

This lattice of string operators plays a crucial role in determining the spectrum of defect operators. In a four-dimensional gauge theory the “defect group” $\Lambda_{\text{root}}^*/\Lambda_{\text{root}}$ (where Λ_{root} is the root lattice of the gauge algebra and Λ_{root}^* is its dual) organizes the set of charged operators that cannot be screened. On a basic level, the dual lattice tells us about the non-trivial line defects that the theory supports. The geometric understanding of the origin of these lattices from the brane picture (at least for SCFTs) can be lifted to a similar defect group for six-dimensional theories [22], where now Λ_{string} is the charge lattice of tensionless BPS strings and $\Lambda_{\text{string}}^*$ is the lattice of string defects that the theory supports. The six-dimensional defect group is then given by $\Lambda_{\text{string}}^*/\Lambda_{\text{string}}$, which determines the strings charged under self-dual two-forms that cannot be screened.

4.2.1 Anomaly polynomial

The anomaly polynomial, I_8 , capturing the perturbative ’t Hooft anomalies for continuous symmetries of six-dimensional $\mathcal{N} = (1, 0)$ theories has been well studied in [63–65] and can be computed from the low-energy EFT on the tensor branch. The necessary condition is that the tensor branch EFT contains the appropriate Green-Schwarz (GS) coupling to cancel reducible gauge anomalies. That is, $I_8 \sim (I_4^{\text{gauge}})^2$ where $I_4^{\text{gauge}} = 1/2 \text{tr}_\lambda(F_g \wedge F_g)$, F_g is the field strength of the gauge field, and λ is a representation of the gauge algebra. Let us define the Dirac pairing of BPS strings,

$$C_{ij} = -\Omega_{ij}, \quad (4.12)$$

where C_{ij} is the same intersection pairing introduced in (4.8). Then the GS coupling [66, 67] takes the form

$$S_{\text{GS}} = \int_{M_6} C_{ij} B_2^i \wedge I_4^j. \quad (4.13)$$

S_{GS} couples the tensors to the gauge fields, but I_4^i also contains characteristic classes of the global symmetries like the first Pontryagin class of the tangent bundle $p_1(T)$, as well as the second Chern class of the $\text{SU}(2)_{R_I}$ -symmetry bundle $c_2(I)$.

Let us be more specific:

$$I_4^i = \frac{1}{4} \text{Tr}(F_i \wedge F_i) + y^i c_2(I) - K^i p_1(T), \quad (4.14)$$

where $\text{Tr} \cong \text{tr}_\lambda / \text{Ind}(\lambda)$ is the normalized trace over the index of the representation λ , and F_i is the field strength of the gauge field associated to the D7-brane wrapping A_i ; keeping in mind that this can be the trivial gauge algebra as well. In addition we have that for a one-instanton

background $\int_{\Sigma_4} \frac{1}{4} \text{Tr}(F \wedge F) = 1$ for a closed $\Sigma_4 \subset M_6$. y^i, K^i are coefficients such that also mixed gauge-global anomalies are canceled, this is due to the fact that six-dimensional SCFTs do not have two-form conserved currents [68]. This fixes

$$y_i = (C^{-1})^{ij} r_j, \quad r_i = h_{\mathfrak{g}_i}^\vee, \quad (4.15)$$

where $h_{\mathfrak{g}_i}^\vee$ is the dual Coxeter number of the gauge algebra \mathfrak{g}_i . In addition,

$$K^i = (C^{-1})^{ij} (2 - C_{jj}). \quad (4.16)$$

The GS contribution to the anomaly polynomial then reads

$$I_{\text{GS}} = \frac{1}{2} C_{ij} I_4^i I_4^j. \quad (4.17)$$

The origin of I_{GS} from the IIB background was proposed in [64]. This comes in term of a formal twelve-form which we then integrate over the IIB base \mathcal{B} :

$$I_{\text{GS}} = -\frac{1}{2} \int_{\mathcal{B}} Z^2, \quad dF_5 = Z, \quad (4.18)$$

where F_5 is the five-form flux, and [69]

$$Z = \frac{1}{4} \left(c_1(\mathcal{B}) \wedge p_1(T) + \sum_i \text{Tr}(F_i \wedge F_i) \wedge \beta_i \right). \quad (4.19)$$

$c_1(\mathcal{B})$ is the first Chern class of the base, and we have the relation with the anticanonical bundle of \mathcal{B} ,

$$\int_{\mathcal{B}} c_1(\mathcal{B}) \wedge \beta_i = C_{ij} K^j = (2 - C_{ii}), \quad (4.20)$$

along with

$$F_5 = H^i \wedge \beta_i, \quad dH^i = I_4^i, \quad -C_{ij} I^j = \int_{\mathcal{B}} Z \wedge \beta_i, \quad Z = I_4^i \wedge \beta_i. \quad (4.21)$$

We have assumed that dH^i also contains a term proportional to $c_2(R)$, which is necessary for the mixed anomaly cancellation. On the other hand it is not directly visible from the IIB geometric construction because the R-symmetry is not manifest. Plugging (4.21) in (4.18) we get (4.13).

The GS contribution can be also derived from the world-volume action of the D7-branes where the following term should be present:

$$\int_{M_6 \times A_i} C_4 \wedge I^i = \int_{M_6 \times A_i} B_2^j \wedge \beta_j \wedge I^i = \int_{M_6} C_{ij} B_2^i \wedge I^j \quad (4.22)$$

In case of D7-branes the contribution proportional to $\text{Tr}(F_i \wedge F_i)$ and $p_1(T)$ come from the Wess-Zumino term,

$$S_{D7}^{\text{WZ}} = \mu_7 \int_{M_8} \text{Tr} \left[\sum_n C_n \wedge e^{\mathcal{F}} \right]_8, \quad (4.23)$$

where we ignore the dependence on the scalar fields parameterizing the orthogonal directions.

4.2.2 Anomaly inflow for BPS strings and surface defects

As we anticipated, the D3-branes wrapping A_i will provide the BPS strings charged under B_2^i . On the other hand, the D3-branes wrapping non-compact cycles B^i realize the $\mathcal{N} = (0, 4)$ surface defects in the theory [22]. Since both objects are D3-branes, they source additional terms in F_5 :

$$dF_5 = Z + Q^i (\delta^{(4)}(\mathbf{x}^\perp) d\mathbf{x}^\perp + \chi_4(N\Sigma)) \wedge \beta_i + q_i (\delta^{(4)}(\mathbf{x}^\perp) d\mathbf{x}^\perp + \chi_4(N\Sigma)) \wedge \alpha^i \equiv Z' \quad (4.24)$$

where Q^i are the BPS string charges and q_i are the number of defects. \mathbf{x}^\perp are the coordinates of the space $\mathbb{R}_4^\perp \subset M_6$ perpendicular to the BPS strings and surface defects in the six-dimensional space-time. The tangent bundle TM_6 of the background splits into the tangent bundle $T\Sigma$ and the normal bundle $N\Sigma$ (with structure group $SO(4)$) of the defect submanifold Σ . So, as in [70],

$$\begin{aligned} \chi_4(N\Sigma) &= c_2(L) - c_2(R), \\ p_1(TM_6) &= p_1(T\Sigma) + p_1(N\Sigma) = p_1(T\Sigma) - 2(c_2(L) + c_2(R)). \end{aligned} \quad (4.25)$$

The surface defect is a D3 probe in the geometric F-theory setup, which in a string theory background can receive anomaly contributions from the bulk theory by inflow. Placing the probe brane in the string theory background produces a bulk anomaly for a given symmetry. This anomaly is then canceled by an anomaly for the probe brane [71, 72]. We can apply the same logic here. We need to integrate the anomaly polynomial in the presence of the D3 brane probe source given by (4.24). We can either start from IIB or directly from six dimensions. Only the reducible part will contribute I_{GS} to the inflow:

$$\int_{\mathbb{R}_4^\perp \times \mathcal{B}} I_{GS} = - \int_{\mathbb{R}_4^\perp \times \mathcal{B}} \frac{1}{2} (Z')^2 \supset - \int_{\mathcal{B}} I_4^i \wedge \beta_i \wedge (Q^j \beta_j + q_j \alpha^j) = C_{ij} I_4^i Q^j - q_j \delta_i^j I_4^i. \quad (4.26)$$

The first term of (4.26) would now reproduce the one for the BPS strings computed in [70]. But let us focus on the inflow on the defect only, neglecting the inflow contributions on the strings, setting $Q^i = 0$. Plugging in (4.14) and (4.15),

$$\mathcal{I}_4(Q^i = 0) = -q_i (C^{-1})^{ij} r_j c_2(I). \quad (4.27)$$

We need to convert the $SU(2)_{R_I}$ into the $(0, 2)$ $U(1)_r$ superconformal R-symmetry, and for this we use the result of [30, (4.28)],⁵

$$a_\Sigma = 3k_r - \frac{k_g}{2}, \quad r = (R - 2I), \quad (4.28)$$

recalling the definition of k_r in (3.47).

The $SU(2)_{R_I}$ vector bundle, V_I , splits in terms of its Cartan line bundle L_I as $V_I = L_I \oplus L_I^\vee$. This implies that

$$c_2(I) = -c_1(L_I)^2 = -4c_1(r)^2. \quad (4.29)$$

⁵Note that the second equality in (4.28) is slightly different from [30, (4.28)], since we are using half-integral charges with respect to R, I . We thus remove a factor of 2 in the formula [30, (4.28)].

The factor of 4 comes from (4.28); we ignored the contribution from $c_2(R)$ since it vanishes when $Q^i = 0$. In the anomaly polynomial we have,

$$K_I c_2(I) = -4K_I c_1(r)^2 = \frac{k_r}{2} c_1(r)^2, \quad K_I = -q_i (C^{-1})^{ij} r_j, \quad (4.30)$$

which implies that

$$k_r = -8K_I \quad (4.31)$$

The inflow contribution to the surface defect a_Σ anomaly of a generic six-dimensional SCFT is then

$$a_\Sigma = 24q_i (C^{-1})^{ij} r_j. \quad (4.32)$$

In the case where C_{ij} is the Cartan matrix of $\mathfrak{su}(N)$ and r_i are the ranks of the $\mathfrak{su}(r_i)$ gauge nodes of the six-dimensional linear quiver in the tensor branch, the a_Σ anomaly we just obtained in (4.32) matches the gravity computation (3.38).

5 Discussion

In this work, we have characterized the probe limit of large $\mathcal{N} = (0, 4)$ two-dimensional superconformal defects in six-dimensional $\mathcal{N} = (0, 1)$ SCFTs at large N . We have constructed BPS solutions for embedding AdS₃ probe D4-branes in AdS₇ × M₃ solutions of type IIA SUGRA with non-trivial Romans mass [12]. For these probe brane embeddings, we have computed the probe brane contribution to the holographic EE of a spherical region in the dual field theory, the probe brane on-shell action for various AdS₃ boundary geometries, and the two-dimensional gravitational anomaly coming from the probe WZ action. The defect EE and on-shell action uniquely fix the independent defect Weyl anomalies a_Σ and d_2 in eq. (3.38) at large N , while the gravitational anomaly provides a subleading correction to a_Σ in eq. (3.57). These results provide novel holographic predictions for universal quantities that are crucial for the study of the ubiquitous string-like defects in six-dimensional SCFTs.

With our holographic predictions for defect anomalies in hand, section 4 focused on computations in field theory to verify our results by utilizing the various string theoretic construction at our disposal. In particular on the field theory side, we found that the expectation value of a circular Wilson loop in $\mathcal{N} = 1$ SYM theory on S⁵ computed using supersymmetric localization agreed exactly with the holographic computation of the on-shell action of a probe D4-brane wrapping S¹ × S¹ at the conformal boundary of AdS₃. This match mirrors similar computations done for Wilson surface operators in A_{N-1} six-dimensional $\mathcal{N} = (0, 2)$ SCFTs, e.g [21]. In string theoretic constructions, we were able to compute defect 't Hooft anomalies using inflow arguments. Working in IIB, we showed that D3-branes wrapping non-compact cycles receive a contribution from inflow to the R-anomaly in their defect four-form anomaly polynomial that, using the non-perturbative relations between defect 't Hooft and Weyl anomalies in [30], matches the leading large N results for a_Σ obtained using probe brane holography.

The inflow contribution provides the leading order contribution of a_Σ at large N and r_i and we argue that inflow captures the bulk-defects modes. On the other hand the

subleading contribution coming from the Wess-Zumino action of the brane is reproduced by the gravitational anomaly of the 2d quiver description of the system with the defect inserted, which has been derived from the NS5-D2-D4-D6-D8 brane system. The 2d quiver gravitational anomaly does not capture the inflow term and the anomaly inflow does not capture the gravitational anomaly contribution to a_Σ . For this reason, we argue that the 2d quiver describes the intrinsic modes of the defect and the anomaly inflow the bulk-defect degrees of freedom. The latter are leading whereas the former are subleading at large N, r_i .

Acknowledgments

We thank J. Heckman and H. Shimizu for their initial involvement in this paper, which is seeing the light after an unusually long gestation. We express our thanks to Y. Tachikawa for useful comments on the draft. This work is supported in part by the INFN. The work of FA is supported in part by the Italian MUR Departments of Excellence grant 2023-2027 “Quantum Frontiers”. NM is partially supported by the MUR-PRIN grant No. 2022NY2MXY. AT is supported in part by MUR-PRIN contract 2022YZ5BA2.

A Coordinate transformations

Let’s consider the flat Euclidean geometry

$$ds^2 = \delta_{\mu\nu} dx^\mu dx^\nu \tag{A.1}$$

where $\mu, \nu = 1, \dots, 6$. We start from a flat defect in the x^5 - x^6 plane situated at $x^1 = x^2 = x^3 = x^4 = 0$. Consider the conformal transformation $x^\mu \rightarrow \tilde{x}^\mu(x)$ that leaves \mathbb{R}^6 invariant but maps the defect submanifold from $\mathbb{R}^2 \rightarrow \mathbb{S}^2$ with radius R :

$$\tilde{x}^1 = R \frac{4|x|^2 - R^2}{R^2 + 4|x|^2 + 4Rx^1}, \quad \tilde{x}^a = 4R^2 \frac{x^a}{R^2 + 4|x|^2 + 4Rx^1}, \tag{A.2}$$

where $a = 2, \dots, 6$ with inverse transformation

$$x^1 = R \frac{R^2 - |\tilde{x}|^2}{2((R - \tilde{x}^1)^2 + \delta_{bc} \tilde{x}^b \tilde{x}^c)}, \quad x^a = R^2 \frac{\tilde{x}^a}{(R - \tilde{x}^1)^2 + \delta_{bc} \tilde{x}^b \tilde{x}^c}. \tag{A.3}$$

The effect of this transformation is to map eq. (A.1) to

$$ds^2 = \frac{R^4}{((R - \tilde{x}^1)^2 + \delta_{bc} \tilde{x}^b \tilde{x}^c)^2} \delta_{\mu\nu} d\tilde{x}^\mu d\tilde{x}^\nu. \tag{A.4}$$

Importantly the hyperplane $x^1 = \dots = x^4 = 0$ is mapped to $\tilde{x}^2 = \tilde{x}^3 = \tilde{x}^4 = 0$ with $\delta_{\mu\nu} \tilde{x}^\mu \tilde{x}^\nu = R^2$.

To make the defect geometry a bit clearer, use $(\tilde{x}^1)^2 = R^2 - (\tilde{x}^5)^2 - (\tilde{x}^6)^2$ and $\tilde{x}^2 = \tilde{x}^3 = \tilde{x}^4 = 0$ to write the image of the line element of the defect submanifold geometry under the conformal map as

$$ds^2|_\Sigma = R^2 \frac{(R^2 - (\tilde{x}^6)^2)(d\tilde{x}^5)^2 + (R^2 - (\tilde{x}^5)^2)(d\tilde{x}^6)^2 + 2\tilde{x}^5 \tilde{x}^6 d\tilde{x}^5 d\tilde{x}^6}{4(R^2 - (\tilde{x}^5)^2 - (\tilde{x}^6)^2) \left(R - \sqrt{R^2 - (\tilde{x}^5)^2 - (\tilde{x}^6)^2} \right)^2}. \tag{A.5}$$

Then, using the coordinate transformation

$$\tilde{x}^5 = R \sin \Theta \sin \Phi, \quad \tilde{x}^6 = R \sin \Theta \cos \Phi \quad (\text{A.6})$$

we find

$$ds^2|_{\Sigma} = \frac{R^2}{16 \sin^4 \Theta / 2} (d\Theta^2 + \sin^2 \Theta d\Phi^2), \quad (\text{A.7})$$

where the conformal factor can be removed by a residual $\text{SO}(2, 2)$ transformation. So, the defect submanifold embedding now takes the form $\mathbb{S}^2 \hookrightarrow \mathbb{R}^6$.

Since we are ultimately interested in studying the geometry of the probe brane dual to this defect, we write the AdS_7 metric as (3.31), with

$$\begin{aligned} ds_{\mathbb{H}^5}^2 &= d\rho^2 + \sinh^2 \rho d\Omega_4^2, \\ d\Omega_4^2 &= d\zeta^2 + \sin^2 \zeta d\tilde{\Omega}_2^2 + \cos^2 \zeta d\chi^2, \\ d\tilde{\Omega}_2^2 &= d\tilde{\theta}^2 + \sin^2 \tilde{\theta} d\tilde{\phi}^2. \end{aligned} \quad (\text{A.8})$$

Starting from eq. (A.1), we first map to polar coordinates with

$$\begin{aligned} x^1 &= \varrho \cos \zeta \cos \chi, & x^2 &= \varrho \cos \zeta \sin \chi, \\ x^3 &= \varrho \sin \zeta \sin \tilde{\theta} \sin \tilde{\phi}, & x^4 &= \varrho \sin \zeta \sin \tilde{\theta} \cos \tilde{\phi}, & x^5 &= \varrho \sin \zeta \cos \tilde{\theta}, \end{aligned} \quad (\text{A.9})$$

which brings us to

$$ds_6^2 = d\varrho^2 + \varrho^2 d\Omega_4^2 + (dx^6)^2. \quad (\text{A.10})$$

Now, we can map to $\mathbb{H}^5 \times \mathbb{S}^1$ by

$$\varrho = \frac{L \sinh \rho}{\cosh \rho - \cos \varphi}, \quad x^6 = \frac{L \sin \varphi}{\cosh \rho - \cos \varphi}, \quad (\text{A.11})$$

which gives

$$ds_6^2 = \frac{L^2}{(\cosh \rho - \cos \varphi)^2} (d\rho^2 + \sinh^2 \rho d\Omega_4^2 + d\varphi^2). \quad (\text{A.12})$$

Stripping off the overall conformal factor, we can extend this into the bulk with a formula similar to (3.11):

$$\begin{aligned} \varrho &= \frac{\cosh \sigma \sinh \rho}{\cosh \sigma \cosh \rho + \sinh \sigma \cos \varphi}, & x^6 &= \frac{\sinh r \sin \varphi}{\cosh \sigma \cosh \rho + \sinh \sigma \cos \varphi}, \\ z &= \frac{1}{\cosh \sigma \cosh \rho + \sinh \sigma \cos \varphi}. \end{aligned} \quad (\text{A.13})$$

This turns $(dz^2 + d\varrho^2 + \varrho^2 d\Omega_4^2 + dx_6^2)/z^2$ into eq. (3.31). Figure 3 illustrates this coordinate change. The defect wraps the $\mathbb{S}^2 \hookrightarrow \mathbb{H}_5$ at the conformal boundary of \mathbb{H}_5 at $\rho \rightarrow \infty$, $\zeta = \pi/2$. The probe brane wraps $\{\rho, \tilde{\theta}, \tilde{\phi}\}$ in the bulk AdS_7 geometry and an \mathbb{S}^2 in the internal space.

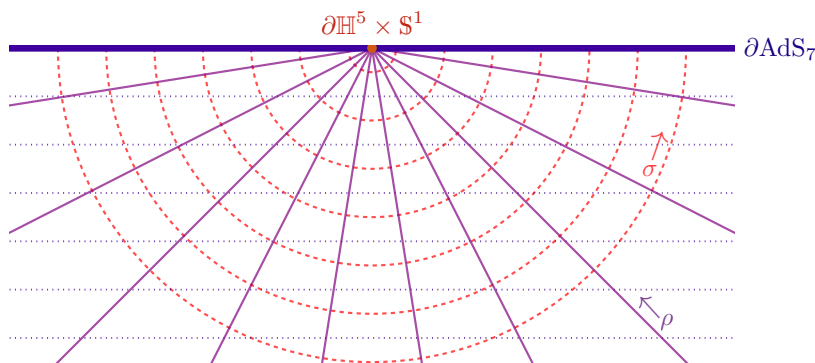


Figure 3. Starting from the flat \mathbb{R}^6 slicing (horizontal blue dotted lines) of AdS_7 , the map in eqs. (A.9) and (A.11) brings us to $\mathbb{H}_5 \times \mathbb{S}^1$ sliced AdS_7 . The conformal boundary ∂AdS_7 in this new coordinatization can be reached by taking either $\sigma \rightarrow \infty$ at fixed ρ which lands in the bulk of \mathbb{H}_5 or $\rho \rightarrow \infty$ at fixed σ which simultaneously takes us to $\partial\mathbb{H}_5 \times \mathbb{S}^1$.

We can follow a similar map that brought us to a spherical defect in $\mathbb{H}_5 \times \mathbb{S}^1$ to bring us to a defect wrapping $\mathbb{S}^1 \times \mathbb{S}^1$ in $\mathbb{S}^5 \times \mathbb{S}^1$. We start with eq. (A.10), and instead of eq. (A.11), we take

$$\varrho = \frac{L \sin \varsigma}{\cosh \tau - \cos \varsigma}, \quad x^6 = \frac{L \sinh \tau}{\cosh \tau - \cos \varsigma}, \quad (\text{A.14})$$

which brings us to

$$ds_6^2 = \frac{L^2}{(\cos \varsigma - \cosh \tau)^2} (d\tau^2 + d\varsigma^2 + \sin^2 \varsigma d\Omega_4^2). \quad (\text{A.15})$$

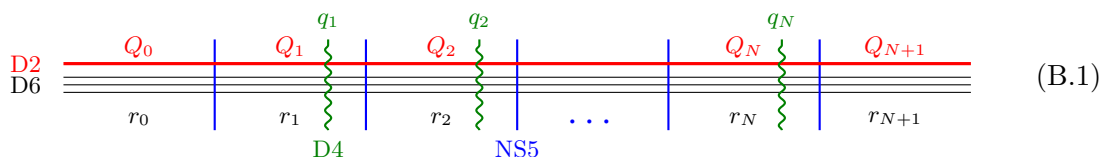
The boundary metric, up to a conformal factor, is now $\mathbb{R} \times \mathbb{S}^5$. Compactifying the τ direction with periodicity $\tau \sim \tau + \beta$ gives us $\mathbb{S}_\beta^1 \times \mathbb{S}^5$. Extending this geometry into the AdS_7 bulk we get

$$ds_7^2 = d\sigma^2 + \cosh^2 \sigma d\tau^2 + \sinh^2 \sigma d\Omega_5^2. \quad (\text{A.16})$$

The probe now wraps (σ, τ) and a great circle at the \mathbb{S}^5 equator as well as the internal \mathbb{S}^2 .

B Two-dimensional quiver gauge theories

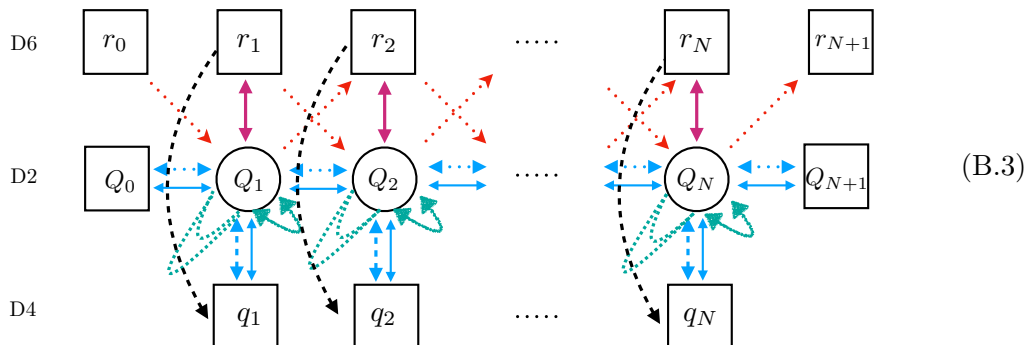
As reviewed in section 2, the six-dimensional theory is realized on the stacks of D6 branes ending on the NS5 branes. The defects we are considering are as in the upper part of figure 2. For completeness we also include the string-like objects realized by D2 branes ending on D4 branes. All in all we end up with the brane intersection in (B.2). For simplicity of the analysis, we do not consider the contribution of the D8 branes in the above configuration, but will briefly comment about their contributions to various anomaly coefficient at the end of this appendix.



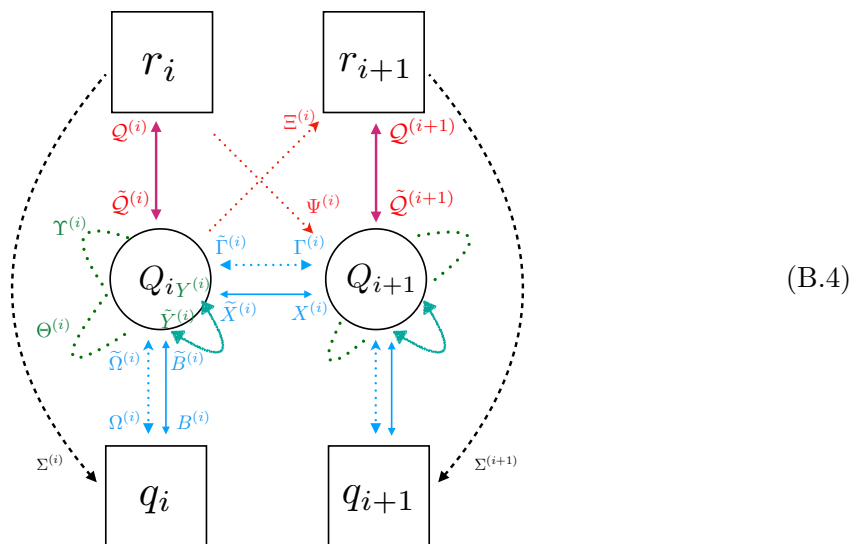
	0	1	2	3	4	5	6	7	8	9
D6	×	×	×	×	×	×	×	-	-	-
D2	×	×	-	-	-	-	×	-	-	-
D4	×	×	-	-	-	-	-	×	×	×
NS5	×	×	×	×	×	×	-	-	-	-

(B.2)

The two-dimensional $\mathcal{N} = (0, 4)$ gauge theory on the D2 brane worldvolume is described by the linear quiver in (B.3), which can be obtained in a similar way to those in [73] and [74].



Let us explain the above quiver diagram as follows. First, we have the circular (gauge) nodes in the center row, which are stacks of Q_i D2 branes (the Q_0 and Q_{N+1} nodes give rise to $U(Q_0)$ and $U(Q_{N+1})$ flavor symmetries respectively). The boxed nodes on the top row are stacks of r_i D6-branes. The boxed nodes in the bottom row are stacks of q_i D4-branes. The length of the row is determined by the number of NS5 branes (N). We take $0 \leq i \leq N + 1$ with $q_0 = q_{N+1} = 0$. We label each field in the quiver as follows.



- The $\mathcal{N} = (0, 4)$ vector multiplet consists an $\mathcal{N} = (0, 2)$ vector multiplet $U^{(i)}$ and an adjoint $\mathcal{N} = (0, 2)$ Fermi multiplet $\Theta^{(i)}$. The vector multiplet $U^{(i)}$ also contains the $\mathcal{N} = (0, 2)$ field strength Fermi multiplet $\Upsilon^{(i)}$. These Fermi multiplets are denoted by dashed green loops in the above diagram.

- The solid green lines are $\mathcal{N} = (0, 4)$ twisted hypermultiplets built out of $\mathcal{N} = (0, 2)$ chirals $(Y^{(i)}, \tilde{Y}^{(i)})$ transforming in the adjoint representation of $U(Q_i)$.
- The horizontal lines connecting the Q_i nodes comprise an $\mathcal{N} = (0, 4)$ hypermultiplet in the bifundamental of $U(Q_i) \times U(Q_{i+1})$ which in $\mathcal{N} = (0, 2)$ language contains chirals $(X^{(i)}, \tilde{X}^{(i)})$ [solid] and Fermi multiplets $(\Gamma^{(i)}, \tilde{\Gamma}^{(i)})$ [dashed].
- The red dashed diagonal lines from the top left corner to bottom right corner are Fermi multiplets Ψ_i charged under $U(r_{i-1}) \times U(Q_i)$. The red dashed diagonal lines from the bottom left corner to top right corner are Fermi multiplets Ξ_i charged under $U(Q_i) \times U(r_{i+1})$.
- The vertical red solid lines are $\mathcal{N} = (0, 4)$ hypermultiplets in the bifundamental of $U(r_i) \times U(Q_i)$ built out of chiral multiplets $(\mathcal{Q}^{(i)}, \tilde{\mathcal{Q}}^{(i)})$.
- The vertical black dashed lines are Fermi multiplets Σ_i charged under $U(r_i) \times U(q_i)$. If there are no D4 branes in the game $q_i = 0$ for all i , then these multiplets are absent.
- The vertical blue lines are $\mathcal{N} = (0, 4)$ hypermultiplets charged in the bifundamental of $U(q_i) \times U(Q_i)$. These multiplets decompose in $\mathcal{N} = (0, 2)$ language as a Fermi multiplet $(\Omega^{(i)}, \tilde{\Omega}^{(i)})$ and chiral multiplet $(B^{(i)}, \tilde{B}^{(i)})$.

The E-term potentials for the various Fermi multiplets and superpotential terms can be written in a similar way as in [73]. Explicitly, the E-terms are

$$\begin{aligned}
 E_{\Theta^{(i)}} &= [Y^{(i)}, \tilde{Y}^{(i)}] + \mathcal{Q}^{(i)} \tilde{\mathcal{Q}}^{(i)} & E_{\Gamma^{(i)}} &= Y^{(i)} X^{(i)} - Y^{(i)} X^{(i-1)} \\
 E_{\tilde{\Gamma}^{(i)}} &= -\tilde{X}^{(i)} Y^{(i)} + \tilde{X}^{(i-1)} Y^{(i)} & E_{\Xi^{(i)}} &= X^{(i)} \mathcal{Q}^{(i+1)} \\
 E_{\Psi^{(i)}} &= \tilde{\mathcal{Q}}^{(i)} X^{(i)} & E_{\Omega^{(i)}} &= Y^{(i)} B^{(i)} - Y^{(i)} B^{(i-1)} \\
 E_{\tilde{\Omega}^{(i)}} &= -\tilde{B}^{(i)} Y^{(i)} + \tilde{B}^{(i-1)} Y^{(i)} & E_{\Sigma^{(i)}} &= \tilde{\mathcal{Q}}^{(i)} B^{(i)}
 \end{aligned} \tag{B.5}$$

and the superpotential terms are

$$\begin{aligned}
 \mathcal{W}_{\Theta^{(i)}} &= \tilde{X}^{(i)} \Theta X^{(i)} - X^{(i-1)} \Theta \tilde{X}^{(i-1)} & \mathcal{W}_{\Gamma^{(i)}} &= \tilde{X}^{(i)} \tilde{Y}^{(i)} \Gamma^{(i)} - \tilde{\Gamma}^{(i-1)} \tilde{Y}^{(i)} X^{(i-1)} \\
 \mathcal{W}_{\tilde{\Gamma}^{(i)}} &= \tilde{\Gamma}^{(i)} \tilde{Y}^{(i)} X^{(i)} - \tilde{X}^{(i-1)} \tilde{Y}^{(i)} \Gamma^{(i-1)} & \mathcal{W}_{\Xi^{(i)}} &= \Xi^{(i)} \tilde{\mathcal{Q}}^{(i+1)} \tilde{X}^{(i)} \\
 \mathcal{W}_{\Psi^{(i)}} &= \Psi^{(i)} \tilde{X}^{(i)} \mathcal{Q}^{(i)} & \mathcal{W}_{\Omega^{(i)}} &= \tilde{B}^{(i)} \tilde{Y}^{(i)} \Omega^{(i)} - \tilde{\Omega}^{(i-1)} \tilde{Y}^{(i)} B^{(i-1)} \\
 \mathcal{W}_{\tilde{\Omega}^{(i)}} &= \tilde{\Omega}^{(i)} \tilde{Y}^{(i)} B^{(i)} - \tilde{B}^{(i-1)} \tilde{Y}^{(i)} \Omega^{(i-1)} & \mathcal{W}_{\Sigma^{(i)}} &= \Sigma^{(i)} \tilde{B}^{(i)} \mathcal{Q}^{(i)}.
 \end{aligned} \tag{B.6}$$

Gauge anomaly cancellation. Let us compute the anomaly for quiver (B.3). First, the gauge anomaly of the $U(1)_i$ subgroup of the $U(Q_i)$ gauge group is given by

$$\text{Tr}(\hat{\gamma}^3 J_{U(1)_i} J_{U(1)_i}) = \sum_{j: \text{chiral}} \mathfrak{q}_j^2 - \sum_{j: \text{Fermi}} \mathfrak{q}_j^2 = 2r_i - r_{i+1} - r_{i-1} \tag{B.7}$$

where $\hat{\gamma}^3$ is the two-dimensional chirality matrix. The gauge anomaly cancellation thus determines $2r_i = r_{i+1} + r_{i-1}$ and is independent of q_i .

This last point deserves a bit of comment. This result is quite different from the gauge anomaly cancellation in [75]. The key difference is that there is an additional pair of chiral

multiplets (B, \tilde{B}) in the construction above that soaks up the anomaly from the $(\Omega, \tilde{\Omega})$ Fermi multiplets which are present in [75]. In the latter case, the n_i are fixed by gauge anomaly cancellation to be $2r_i - r_{i+1} - r_{i-1}$.

The non-abelian gauge anomaly is obviously more involved but we have all the information we need from the list of matter multiplets above:

$$\begin{aligned}
 \text{Tr}(\hat{\gamma}^3 J_{\text{SU}(Q_i)} J_{\text{SU}(Q_i)}) &= (T_{\mathcal{Q}}(\square) + T_{\tilde{\mathcal{Q}}}(\bar{\square}))r_i - T_{\Xi}(\square)r_{i+1} - T_{\Psi}(\bar{\square})r_{i-1} \\
 &\quad + T_X(\square)Q_{i-1} + T_{\tilde{X}}(\bar{\square})Q_{i+1} - T_{\Gamma}(\square)Q_{i-1} + T_{\tilde{\Gamma}}(\bar{\square})Q_{i+1} \\
 &\quad + (T_B(\square) + T_{\tilde{B}}(\bar{\square}))q_i - (T_{\Omega}(\square) + T_{\tilde{\Omega}}(\bar{\square}))q_i \\
 &\quad + T_Y(\mathbf{adj}) + T_{\tilde{Y}}(\mathbf{adj}) - T_{\Upsilon}(\mathbf{adj}) - T_{\Theta}(\mathbf{adj}) \\
 &= r_i - \frac{1}{2}(r_{i+1} + r_{i-1}),
 \end{aligned} \tag{B.8}$$

where $T_F(\mathbf{R})$ denotes the index of the representation \mathbf{R} of $\text{SU}(Q_i)$ in which the field F transforms. We used the convention that the indices of the fundamental and antifundamental representations are $T(\square) = T(\bar{\square}) = \frac{1}{2}$ and that of the adjoint representation is $T(\mathbf{adj}) = Q_i$. This reproduces the abelian gauge anomaly cancellation.

R-symmetry. The two-dimensional $\mathcal{N} = (0, 4)$ gauge theory in question has R-symmetry $\mathfrak{so}(4)_R \cong \mathfrak{su}(2)_R^+ \times \mathfrak{su}(2)_R^-$. Let $R^\pm[F]$ be the charge of the field F under the Cartan subalgebra of $\mathfrak{su}(2)_R^\pm$. The R-charge assignment to each field is constrained by the following conditions:

- We assume the R-charges of the fields are independent of the superscript (i) , and so we write $R^\pm[F^{(i)}] = R^\pm[F]$ for any field F .
- Each superpotential term carries R-charge $R^\pm[\mathcal{W}] = +1$.
- For each Fermi multiplet f , the corresponding E -term has charge $R^\pm[E_f] = R^\pm[f] + 1$.
- $R^\pm[\Upsilon] = 1$ since Υ is in the multiplet that contains the field strength.

As pointed out in [73], the fields $\Gamma^{(i)}$ and $\tilde{\Gamma}^{(i)}$ are singlets under $\mathfrak{su}(2)_R^+ \times \mathfrak{su}(2)_R^-$:

$$R^\pm[\Gamma] = 0, \quad R^\pm[\tilde{\Gamma}] = 0. \tag{B.9}$$

Moreover, as pointed out in [76, 77] and [73, p. 10], it is possible to have a single $\mathcal{N} = (0, 2)$ Fermi multiplet which is consistent with $\mathcal{N} = (0, 4)$ supersymmetry. However, for this to happen, the chiral fermion should be a singlet under $\mathfrak{su}(2)_R^+ \times \mathfrak{su}(2)_R^-$. Thus,

$$R^\pm[\Xi] = 0, \quad R^\pm[\Psi] = 0. \tag{B.10}$$

Taking these into account, we obtain the following R-charge assignment:

	Υ	Θ	Y	\tilde{Y}	X	\tilde{X}	\mathcal{Q}	$\tilde{\mathcal{Q}}$	B	\tilde{B}	Γ	$\tilde{\Gamma}$	Ω	$\tilde{\Omega}$	Ξ	Ψ	Σ
R^+	1	1	1	1	0	0	1	1	0	0	0	0	0	0	0	0	0
R^-	1	-1	0	0	1	1	0	0	1	1	0	0	0	0	0	0	0

(B.11)

SU(2)_D flavor symmetry. Our quiver theory also has an SU(2)_D flavor symmetry that transforms the $\mathcal{N} = (0, 4)$ adjoint twisted hypermultiplet $(Y^{(i)}, \tilde{Y}^{(i)})$ as a doublet for each i . We assign their charges under the SU(2)_D Cartan subalgebra as

$$D[Y^{(i)}] = 1, \quad D[\tilde{Y}^{(i)}] = -1. \quad (\text{B.12})$$

Since the superpotential terms have transform trivially under this symmetry, from (B.6) we find that the consistent charge assignment is as follows:

	Υ	Θ	Y	\tilde{Y}	X	\tilde{X}	\mathcal{Q}	$\tilde{\mathcal{Q}}$	B	\tilde{B}	Γ	$\tilde{\Gamma}$	Ω	$\tilde{\Omega}$	Ξ	Ψ	Σ
D	0	0	1	-1	0	0	0	0	0	0	1	1	1	1	0	0	0

(B.13)

Note that $\Upsilon^{(i)}$ and $\Theta^{(i)}$, residing in the $\mathcal{N} = (0, 4)$ vector multiplet, transform trivially in the SU(2)_D flavor symmetry.

Gravitational, R-symmetry and SU(2)_D anomalies. The four-form anomaly polynomial of the two-dimensional quiver gauge theory contains the following terms:

$$\frac{1}{2}K_{R^+}c_2(R^+) + \frac{1}{2}K_{R^-}c_2(R^-) + \frac{1}{2}K_Dc_2(D) + k_g p_1(T), \quad (\text{B.14})$$

where K_{R^\pm} are R-symmetry anomalies, K_D is the SU(2)_D symmetry anomaly, and k_g is the gravitational anomaly of the quiver theory:

$$\begin{aligned} K_{R^\pm} &= \text{Tr}(\hat{\gamma}^3 J_{\text{SU}(2)_R^\pm} J_{\text{SU}(2)_R^\pm}), & K_D &= \text{Tr}(\hat{\gamma}^3 J_{\text{SU}(2)_D} J_{\text{SU}(2)_D}), & k_g &= \text{Tr} \hat{\gamma}^3 \\ c_2(R^\pm) &= c_2(\text{SU}(2)_R^\pm), & c_2(D) &= c_2(\text{SU}(2)_D), \end{aligned} \quad (\text{B.15})$$

For the R-anomalies, the left moving fermions in the Fermi multiplets ψ contribute $-R[\psi]^2$ and the fermions in the chiral multiplet χ contribute $(R[\chi] - 1)^2$, where $R[X] = R_X$ denotes either $R^+[X]$ or $R^-[X]$. The counting results in

$$\begin{aligned} K_R &= \sum_{i=0}^{N+1} \left[Q_i Q_{i+1} \left((R_X - 1)^2 + (R_{\tilde{X}} - 1)^2 - R_\Gamma^2 - R_{\tilde{\Gamma}}^2 \right) - Q_i r_{i+1} R_\Xi^2 - Q_i r_{i-1} R_\Psi^2 \right] \\ &+ \sum_{i=1}^N q_i \left[Q_i \left((R_B - 1)^2 + (R_{\tilde{B}} - 1)^2 - R_\Omega^2 - R_{\tilde{\Omega}}^2 \right) - r_i R_\Sigma^2 \right] \\ &+ \sum_{i=1}^N Q_i \left[Q_i \left((R_Y - 1)^2 + (R_{\tilde{Y}} - 1)^2 - R_\Upsilon^2 - R_\Theta^2 \right) + r_i (R_\mathcal{Q} - 1)^2 + r_i (R_{\tilde{\mathcal{Q}}} - 1)^2 \right]. \end{aligned} \quad (\text{B.16})$$

Explicitly, using (B.11), we have

$$K_R = \begin{cases} 2 \sum_{i=1}^N r_i Q_i & \text{if } R = R^- \\ 2 \sum_{i=1}^N (q_i - Q_i) Q_i + 2 \sum_{i=0}^N Q_i Q_{i+1} & \text{if } R = R^+. \end{cases} \quad (\text{B.17})$$

On the other hand, the gravitational anomaly can be obtained from by replacing $(R_F - 1)^2$ and R_F^2 in (B.16) by 1 for every field F :

$$k_g = - \sum_{i=1}^N r_i q_i + \sum_{i=1}^N (2r_i - r_{i+1} - r_{i-1}) Q_i = - \sum_{i=1}^N r_i q_i, \quad (\text{B.18})$$

where we have used the gauge anomaly cancellation to obtain the last equality.

Finally, the $SU(2)_D$ anomaly can be computed by replacing $(R_F - 1)^2$ and R_F^2 in (B.16) by $D[F]^2$, where $D[F]$ is the charge of F under the Cartan subalgebra of $SU(2)_D$ given by (B.16) for every field F . The result is

$$K_D = -K_{R^+} = 2 \sum_{i=1}^N (Q_i - q_i) Q_i - 2 \sum_{i=0}^N Q_i Q_{i+1}. \tag{B.19}$$

To summarize, the terms (B.14) in the four-form anomaly polynomial of the two-dimensional quiver theory can be written as

$$\begin{aligned} & \frac{1}{2} K_D [c_2(D) - c_2(R^+)] + \frac{1}{2} K_{R^-} c_2(R^-) + k_g p_1(T) \\ &= \left(\sum_{i=1}^N (Q_i - q_i) Q_i - \sum_{i=0}^N Q_i Q_{i+1} \right) [c_2(D) - c_2(R^+)] \\ &+ \left(\sum_{i=1}^N r_i Q_i \right) c_2(R^-) + \left(- \sum_{i=1}^N r_i q_i \right) p_1(T). \end{aligned} \tag{B.20}$$

It is instructive to compare this result to [70, (2.5)] in the case of $q_i = 0$. According to [70, Page 7], the coefficient of $c_2(R^-)$ in (B.20) coincides with that of $c_2(I)$ in [70], and so we identify our $SU(2)_{\bar{R}}$ with their $SU(2)_I$. Moreover, the coefficient of $[c_2(D) - c_2(R^+)]$ when $q_i = 0$ can be written as $\frac{1}{2} \sum_{i,j=1}^N C_{ij} Q_i Q_j$ where C_{ij} is the Cartan matrix of the A_N algebra. This is in agreement with the coefficient of $c_2(L) - c_2(R)$ of [70, (2.5)] when their η^{ij} is taken to be the Cartan matrix C_{ij} . We thus identify our $SU(2)_D - SU(2)_{\bar{R}}$ with their $SU(2)_L - SU(2)_R$. Finally, we see that for $q_i = 0$ the gravitation anomaly k_g vanishes, in agreement with the coefficient of $p_1(T)$ and $c_2(L) + c_2(R)$ of [70, (2.5)] when η^{ij} is taken to be the Cartan matrix C_{ij} , whose diagonal elements are precisely 2. This is also consistent with (B.19), namely the coefficient of $c_2(D) + c_2(R^+)$ in our anomaly polynomial is zero. This leads to the identification of our $SU(2)_D + SU(2)_{\bar{R}}$ with their $SU(2)_L + SU(2)_R$. The R-symmetry of the two-dimensional theory in our notation is $SU(2)_{\bar{R}}^+ \times SU(2)_{\bar{R}}$ and in their notation is $SU(2)_R \times SU(2)_I$. We therefore identify

$$SU(2)_{\bar{R}}^- \equiv SU(2)_I, \quad SU(2)_{\bar{R}}^+ \equiv SU(2)_R, \quad SU(2)_D \equiv SU(2)_L, \tag{B.21}$$

in our and their notations, respectively.

We can compute the defect anomaly from the formula (4.28), namely

$$a_\Sigma = 3k_r - \frac{1}{2} k_g. \tag{B.22}$$

Note that the anomaly polynomial (B.14) contains the terms $\frac{1}{2} K_{R^+} c_2(R^+) = -\frac{1}{2} K_{R^+} c_1(r)^2$ and $\frac{1}{2} K_{R^-} c_2(R^-) = -\frac{4}{2} K_{R^-} c_1(r)^2 = -2 K_{R^-} c_1(r)^2$, where we have used the fact that $c_2(R^+) = -c_1(r)^2$ and $c_2(R^-) = c_2(I) = -4c_1(r)^2$; see (B.21), (4.28) and (4.29). Recalling that we adopt the convention $\frac{1}{2} k_r c_1(r)^2$ in the anomaly polynomial, we thus obtain

$$k_r = \begin{cases} -4K_{R^-} & \text{for } SU(2)_{\bar{R}}^- \\ -K_{R^+} & \text{for } SU(2)_{\bar{R}}^+. \end{cases} \tag{B.23}$$

Applying the formulae (B.17) and (B.18), we obtain

$$a_\Sigma = \begin{cases} -24 \sum_{i=1}^N r_i Q_i + \frac{1}{2} \sum_{i=1}^N r_i q_i & \text{if } R = R^- \\ -6 \left(\sum_{i=1}^N (q_i - Q_i) Q_i + \sum_{i=0}^N Q_i Q_{i+1} \right) + \frac{1}{2} \sum_{i=1}^N r_i q_i & \text{if } R = R^+. \end{cases} \quad (\text{B.24})$$

We extract the defect anomaly by setting the BPS string charges $Q_i = 0$.

We finally comment on the insertion of f_i D8-branes, which span the 012345 789 directions, in the brane system which engineers 6d theories intersecting the i -th D6 segment. The extra contribution to 2d quiver gauge theory is provided by D2-D8 states that are $f_i Q_i$ (0, 2) Fermi multiplets.⁶ In addition, the cancellation of the gauge anomalies (B.8) and (B.7) now requires

$$2r_i - r_{i+1} - r_{i-1} - f_i = 0 \quad (\text{B.25})$$

which is equivalent to the 6d irreducible gauge anomaly (proportional to $\text{tr}(F^4)$ in the 6d anomaly polynomial) cancellation condition. All the R-charge assignments are the same as $R_{\Xi(i)}$. Therefore, the K_{R^\pm} and K_D will receive contributions from $f_i Q_i$ (0, 2) Fermi multiplets accordingly. The gravitational anomaly remains unchanged since it explicitly depends on the gauge anomaly cancellation condition (B.18). We conclude that the addition of D8 branes does not change the defect anomaly contribution, but it changes the BPS strings R-symmetries anomalies.

Data Availability Statement. This article has no associated data or the data will not be deposited.

Code Availability Statement. This article has no associated code or the code will not be deposited.

Open Access. This article is distributed under the terms of the Creative Commons Attribution License (CC-BY4.0), which permits any use, distribution and reproduction in any medium, provided the original author(s) and source are credited.

References

- [1] A. Karch and E. Katz, *Adding flavor to AdS/CFT*, *JHEP* **06** (2002) 043 [[hep-th/0205236](#)] [[INSPIRE](#)].
- [2] O. DeWolfe, D.Z. Freedman and H. Ooguri, *Holography and defect conformal field theories*, *Phys. Rev. D* **66** (2002) 025009 [[hep-th/0111135](#)] [[INSPIRE](#)].
- [3] N.R. Constable, J. Erdmenger, Z. Guralnik and I. Kirsch, *Intersecting D-3 branes and holography*, *Phys. Rev. D* **68** (2003) 106007 [[hep-th/0211222](#)] [[INSPIRE](#)].
- [4] A. Karch, B. Robinson and C.F. Uhlemann, *Supersymmetric D3/D7 for holographic flavors on curved space*, *JHEP* **11** (2015) 112 [[arXiv:1508.06996](#)] [[INSPIRE](#)].
- [5] A. Karch, B. Robinson and C.F. Uhlemann, *Precision Test of Gauge-Gravity Duality with Flavor*, *Phys. Rev. Lett.* **115** (2015) 261601 [[arXiv:1509.00013](#)] [[INSPIRE](#)].

⁶The D4-D8 states will not contribute since they are not light 2d degrees of freedom.

- [6] B. Robinson and C.F. Uhlemann, *Supersymmetric D3/D5 for massive defects on curved space*, *JHEP* **12** (2017) 143 [[arXiv:1709.08650](#)] [[INSPIRE](#)].
- [7] E. Witten, *Some comments on string dynamics*, in the proceedings of the *STRINGS 95: Future Perspectives in String Theory*, Los Angeles, U.S.A., March 13–18 (1995) [[hep-th/9507121](#)] [[INSPIRE](#)].
- [8] K.A. Intriligator, *New string theories in six-dimensions via branes at orbifold singularities*, *Adv. Theor. Math. Phys.* **1** (1998) 271 [[hep-th/9708117](#)] [[INSPIRE](#)].
- [9] O.J. Ganor and A. Hanany, *Small E(8) instantons and tensionless noncritical strings*, *Nucl. Phys. B* **474** (1996) 122 [[hep-th/9602120](#)] [[INSPIRE](#)].
- [10] J.J. Heckman, D.R. Morrison and C. Vafa, *On the Classification of 6D SCFTs and Generalized ADE Orbifolds*, *JHEP* **05** (2014) 028 [*Erratum ibid.* **06** (2015) 017] [[arXiv:1312.5746](#)] [[INSPIRE](#)].
- [11] A. Hanany and A. Zaffaroni, *Branes and six-dimensional supersymmetric theories*, *Nucl. Phys. B* **529** (1998) 180 [[hep-th/9712145](#)] [[INSPIRE](#)].
- [12] F. Apruzzi, M. Fazzi, D. Rosa and A. Tomasiello, *All AdS₇ solutions of type II supergravity*, *JHEP* **04** (2014) 064 [[arXiv:1309.2949](#)] [[INSPIRE](#)].
- [13] F. Apruzzi et al., *Six-Dimensional Superconformal Theories and their Compactifications from Type IIA Supergravity*, *Phys. Rev. Lett.* **115** (2015) 061601 [[arXiv:1502.06616](#)] [[INSPIRE](#)].
- [14] S. Cremonesi and A. Tomasiello, *6d holographic anomaly match as a continuum limit*, *JHEP* **05** (2016) 031 [[arXiv:1512.02225](#)] [[INSPIRE](#)].
- [15] D. Gaiotto, *N = 2 dualities*, *JHEP* **08** (2012) 034 [[arXiv:0904.2715](#)] [[INSPIRE](#)].
- [16] D. Gaiotto and J. Maldacena, *The gravity duals of N = 2 superconformal field theories*, *JHEP* **10** (2012) 189 [[arXiv:0904.4466](#)] [[INSPIRE](#)].
- [17] P. Agarwal, I. Bah, K. Maruyoshi and J. Song, *Quiver tails and N = 1 SCFTs from M5-branes*, *JHEP* **03** (2015) 049 [[arXiv:1409.1908](#)] [[INSPIRE](#)].
- [18] S.S. Razamat, E. Sabag, O. Sela and G. Zafrir, *Aspects of 4d supersymmetric dynamics and geometry*, *SciPost Phys. Lect. Notes* **78** (2024) 1 [[arXiv:2203.06880](#)] [[INSPIRE](#)].
- [19] L.F. Alday et al., *Loop and surface operators in N = 2 gauge theory and Liouville modular geometry*, *JHEP* **01** (2010) 113 [[arXiv:0909.0945](#)] [[INSPIRE](#)].
- [20] N. Drukker, D. Gaiotto and J. Gomis, *The Virtue of Defects in 4D Gauge Theories and 2D CFTs*, *JHEP* **06** (2011) 025 [[arXiv:1003.1112](#)] [[INSPIRE](#)].
- [21] H. Mori and S. Yamaguchi, *M5-branes and Wilson surfaces in AdS₇/CFT₆ correspondence*, *Phys. Rev. D* **90** (2014) 026005 [[arXiv:1404.0930](#)] [[INSPIRE](#)].
- [22] M. Del Zotto, J.J. Heckman, D.S. Park and T. Rudelius, *On the Defect Group of a 6D SCFT*, *Lett. Math. Phys.* **106** (2016) 765 [[arXiv:1503.04806](#)] [[INSPIRE](#)].
- [23] C. Herzog, K.-W. Huang and K. Jensen, *Displacement Operators and Constraints on Boundary Central Charges*, *Phys. Rev. Lett.* **120** (2018) 021601 [[arXiv:1709.07431](#)] [[INSPIRE](#)].
- [24] I. Affleck, *Universal Term in the Free Energy at a Critical Point and the Conformal Anomaly*, *Phys. Rev. Lett.* **56** (1986) 746 [[INSPIRE](#)].
- [25] N. Andrei et al., *Boundary and Defect CFT: Open Problems and Applications*, *J. Phys. A* **53** (2020) 453002 [[arXiv:1810.05697](#)] [[INSPIRE](#)].

- [26] I. Bah, F. Bonetti, R. Minasian and E. Nardoni, *Anomaly Inflow for M5-branes on Punctured Riemann Surfaces*, *JHEP* **06** (2019) 123 [[arXiv:1904.07250](#)] [[INSPIRE](#)].
- [27] K. Jensen, A. O’Bannon, B. Robinson and R. Rodgers, *From the Weyl Anomaly to Entropy of Two-Dimensional Boundaries and Defects*, *Phys. Rev. Lett.* **122** (2019) 241602 [[arXiv:1812.08745](#)] [[INSPIRE](#)].
- [28] S. Deser and A. Schwimmer, *Geometric classification of conformal anomalies in arbitrary dimensions*, *Phys. Lett. B* **309** (1993) 279 [[hep-th/9302047](#)] [[INSPIRE](#)].
- [29] K. Jensen and A. O’Bannon, *Constraint on Defect and Boundary Renormalization Group Flows*, *Phys. Rev. Lett.* **116** (2016) 091601 [[arXiv:1509.02160](#)] [[INSPIRE](#)].
- [30] Y. Wang, *Surface defect, anomalies and b-extremization*, *JHEP* **11** (2021) 122 [[arXiv:2012.06574](#)] [[INSPIRE](#)].
- [31] M. Billò, V. Gonçalves, E. Lauria and M. Meineri, *Defects in conformal field theory*, *JHEP* **04** (2016) 091 [[arXiv:1601.02883](#)] [[INSPIRE](#)].
- [32] L. Bianchi and M. Lemos, *Superconformal surfaces in four dimensions*, *JHEP* **06** (2020) 056 [[arXiv:1911.05082](#)] [[INSPIRE](#)].
- [33] N. Drukker, M. Probst and M. Trépanier, *Defect CFT techniques in the 6d $\mathcal{N} = (2, 0)$ theory*, *JHEP* **03** (2021) 261 [[arXiv:2009.10732](#)] [[INSPIRE](#)].
- [34] N. Kobayashi, T. Nishioka, Y. Sato and K. Watanabe, *Towards a C-theorem in defect CFT*, *JHEP* **01** (2019) 039 [[arXiv:1810.06995](#)] [[INSPIRE](#)].
- [35] E. D’Hoker, J. Estes, M. Gutperle and D. Krym, *Exact Half-BPS Flux Solutions in M-theory. I: Local Solutions*, *JHEP* **08** (2008) 028 [[arXiv:0806.0605](#)] [[INSPIRE](#)].
- [36] G. Dibitetto and N. Petri, *6d surface defects from massive type IIA*, *JHEP* **01** (2018) 039 [[arXiv:1707.06154](#)] [[INSPIRE](#)].
- [37] Y. Lozano, N.T. Macpherson, C. Nunez and A. Ramirez, *AdS₃ solutions in massive IIA, defect CFTs and T-duality*, *JHEP* **12** (2019) 013 [[arXiv:1909.11669](#)] [[INSPIRE](#)].
- [38] Y. Lozano, N.T. Macpherson, N. Petri and C. Risco, *New AdS₃/CFT₂ pairs in massive IIA with (0, 4) and (4, 4) supersymmetries*, *JHEP* **09** (2022) 130 [[arXiv:2206.13541](#)] [[INSPIRE](#)].
- [39] D. Gaiotto and A. Tomasiello, *Holography for (1, 0) theories in six dimensions*, *JHEP* **12** (2014) 003 [[arXiv:1404.0711](#)] [[INSPIRE](#)].
- [40] F. Apruzzi and M. Fazzi, *AdS₇/CFT₆ with orientifolds*, *JHEP* **01** (2018) 124 [[arXiv:1712.03235](#)] [[INSPIRE](#)].
- [41] A. Karch, A. O’Bannon and K. Skenderis, *Holographic renormalization of probe D-branes in AdS/CFT*, *JHEP* **04** (2006) 015 [[hep-th/0512125](#)] [[INSPIRE](#)].
- [42] H. Casini, M. Huerta and R.C. Myers, *Towards a derivation of holographic entanglement entropy*, *JHEP* **05** (2011) 036 [[arXiv:1102.0440](#)] [[INSPIRE](#)].
- [43] K. Jensen and A. O’Bannon, *Holography, Entanglement Entropy, and Conformal Field Theories with Boundaries or Defects*, *Phys. Rev. D* **88** (2013) 106006 [[arXiv:1309.4523](#)] [[INSPIRE](#)].
- [44] L.-Y. Hung, R.C. Myers, M. Smolkin and A. Yale, *Holographic Calculations of Renyi Entropy*, *JHEP* **12** (2011) 047 [[arXiv:1110.1084](#)] [[INSPIRE](#)].
- [45] S. Ryu and T. Takayanagi, *Holographic derivation of entanglement entropy from AdS/CFT*, *Phys. Rev. Lett.* **96** (2006) 181602 [[hep-th/0603001](#)] [[INSPIRE](#)].

- [46] R. Rodgers, *Holographic entanglement entropy from probe M-theory branes*, *JHEP* **03** (2019) 092 [[arXiv:1811.12375](#)] [[INSPIRE](#)].
- [47] S.P. Kumar and D. Silvani, *Entanglement of heavy quark impurities and generalized gravitational entropy*, *JHEP* **01** (2018) 052 [[arXiv:1711.01554](#)] [[INSPIRE](#)].
- [48] J. Estes et al., *Wilson Surface Central Charge from Holographic Entanglement Entropy*, *JHEP* **05** (2019) 032 [[arXiv:1812.00923](#)] [[INSPIRE](#)].
- [49] B. Assel, D. Cassani and D. Martelli, *Localization on Hopf surfaces*, *JHEP* **08** (2014) 123 [[arXiv:1405.5144](#)] [[INSPIRE](#)].
- [50] B. Assel et al., *The Casimir Energy in Curved Space and its Supersymmetric Counterpart*, *JHEP* **07** (2015) 043 [[arXiv:1503.05537](#)] [[INSPIRE](#)].
- [51] N. Bobev, M. Bullimore and H.-C. Kim, *Supersymmetric Casimir Energy and the Anomaly Polynomial*, *JHEP* **09** (2015) 142 [[arXiv:1507.08553](#)] [[INSPIRE](#)].
- [52] A. Chalabi, A. O'Bannon, B. Robinson and J. Sisti, *Central charges of 2d superconformal defects*, *JHEP* **05** (2020) 095 [[arXiv:2003.02857](#)] [[INSPIRE](#)].
- [53] C. Meneghelli and M. Trépanier, *Bootstrapping string dynamics in the 6d $\mathcal{N} = (2, 0)$ theories*, *JHEP* **07** (2023) 165 [[arXiv:2212.05020](#)] [[INSPIRE](#)].
- [54] O. Aharony and Y. Tachikawa, *A holographic computation of the central charges of $d = 4$, $N = 2$ SCFTs*, *JHEP* **01** (2008) 037 [[arXiv:0711.4532](#)] [[INSPIRE](#)].
- [55] M. Del Zotto, J.J. Heckman, A. Tomasiello and C. Vafa, *6d Conformal Matter*, *JHEP* **02** (2015) 054 [[arXiv:1407.6359](#)] [[INSPIRE](#)].
- [56] J. Gomis and F. Passerini, *Holographic Wilson Loops*, *JHEP* **08** (2006) 074 [[hep-th/0604007](#)] [[INSPIRE](#)].
- [57] J. Gomis and F. Passerini, *Wilson Loops as D3-Branes*, *JHEP* **01** (2007) 097 [[hep-th/0612022](#)] [[INSPIRE](#)].
- [58] J.A. Minahan, A. Nedelin and M. Zabzine, *5D super Yang-Mills theory and the correspondence to AdS_7/CFT_6* , *J. Phys. A* **46** (2013) 355401 [[arXiv:1304.1016](#)] [[INSPIRE](#)].
- [59] J.A. Minahan, *Matrix models for 5d super Yang-Mills*, *J. Phys. A* **50** (2017) 443015 [[arXiv:1608.02967](#)] [[INSPIRE](#)].
- [60] H.-C. Kim, J. Kim and S. Kim, *Instantons on the 5-sphere and M5-branes*, [arXiv:1211.0144](#) [[INSPIRE](#)].
- [61] J. Kallen, J.A. Minahan, A. Nedelin and M. Zabzine, *N^3 -behavior from 5D Yang-Mills theory*, *JHEP* **10** (2012) 184 [[arXiv:1207.3763](#)] [[INSPIRE](#)].
- [62] J.J. Heckman, D.R. Morrison, T. Rudelius and C. Vafa, *Atomic Classification of 6D SCFTs*, *Fortsch. Phys.* **63** (2015) 468 [[arXiv:1502.05405](#)] [[INSPIRE](#)].
- [63] C. Cordova, T.T. Dumitrescu and K. Intriligator, *Anomalies, renormalization group flows, and the a-theorem in six-dimensional $(1, 0)$ theories*, *JHEP* **10** (2016) 080 [[arXiv:1506.03807](#)] [[INSPIRE](#)].
- [64] K. Ohmori, H. Shimizu, Y. Tachikawa and K. Yonekura, *Anomaly polynomial of general 6d SCFTs*, *PTEP* **2014** (2014) 103B07 [[arXiv:1408.5572](#)] [[INSPIRE](#)].
- [65] K. Intriligator, *6d, $\mathcal{N} = (1, 0)$ Coulomb branch anomaly matching*, *JHEP* **10** (2014) 162 [[arXiv:1408.6745](#)] [[INSPIRE](#)].

- [66] M.B. Green, J.H. Schwarz and P.C. West, *Anomaly Free Chiral Theories in Six-Dimensions*, *Nucl. Phys. B* **254** (1985) 327 [[INSPIRE](#)].
- [67] A. Sagnotti, *A note on the Green-Schwarz mechanism in open string theories*, *Phys. Lett. B* **294** (1992) 196 [[hep-th/9210127](#)] [[INSPIRE](#)].
- [68] C. Cordova, T.T. Dumitrescu and K. Intriligator, *2-Group Global Symmetries and Anomalies in Six-Dimensional Quantum Field Theories*, *JHEP* **04** (2021) 252 [[arXiv:2009.00138](#)] [[INSPIRE](#)].
- [69] V. Sadov, *Generalized Green-Schwarz mechanism in F theory*, *Phys. Lett. B* **388** (1996) 45 [[hep-th/9606008](#)] [[INSPIRE](#)].
- [70] H. Shimizu and Y. Tachikawa, *Anomaly of strings of 6d $\mathcal{N} = (1, 0)$ theories*, *JHEP* **11** (2016) 165 [[arXiv:1608.05894](#)] [[INSPIRE](#)].
- [71] D. Freed, J.A. Harvey, R. Minasian and G.W. Moore, *Gravitational anomaly cancellation for M theory five-branes*, *Adv. Theor. Math. Phys.* **2** (1998) 601 [[hep-th/9803205](#)] [[INSPIRE](#)].
- [72] H. Kim and P. Yi, *D-brane anomaly inflow revisited*, *JHEP* **02** (2012) 012 [[arXiv:1201.0762](#)] [[INSPIRE](#)].
- [73] D. Tong, *The holographic dual of $AdS_3 \times S^3 \times S^3 \times S^1$* , *JHEP* **04** (2014) 193 [[arXiv:1402.5135](#)] [[INSPIRE](#)].
- [74] B. Haghighat et al., *M-Strings*, *Commun. Math. Phys.* **334** (2015) 779 [[arXiv:1305.6322](#)] [[INSPIRE](#)].
- [75] A. Gadde et al., *6d String Chains*, *JHEP* **02** (2018) 143 [[arXiv:1504.04614](#)] [[INSPIRE](#)].
- [76] E. Witten, *Sigma models and the ADHM construction of instantons*, *J. Geom. Phys.* **15** (1995) 215 [[hep-th/9410052](#)] [[INSPIRE](#)].
- [77] P. Putrov, J. Song and W. Yan, *(0, 4) dualities*, *JHEP* **03** (2016) 185 [[arXiv:1505.07110](#)] [[INSPIRE](#)].